



BENEMÉRITA UNIVERSIDAD AUTÓNOMA DE PUEBLA

INSTITUTO DE FÍSICA "LUIS RIVERA TERRAZAS"

"FRACTAL TO NON-FRACTAL
MORPHOLOGICAL TRANSITIONS IN
STOCHASTIC GROWTH PROCESSES"

TESIS

QUE PARA OBTENER EL GRADO DE

DOCTOR EN CIENCIAS
(FÍSICA)

PRESENTA:
M.C. JOSÉ ROBERTO NICOLÁS CARLOCK

ASESOR:
DR. JOSÉ LUIS CARRILLO ESTRADA

CO-ASESOR:
DR. VÍCTOR DOSSETTI ROMERO

JUNIO 2017

Contents

Acknowledgements	iii
Abstract	v
Publications	ix
Introduction	xi
1 Fractal Growth Models	1
1.1 Stochastic growth	1
1.1.1 DLA and BA models	1
1.1.2 Mean-Field (MF) aggregation model	3
1.1.3 Dielectric Breakdown Model (DBM)	3
1.2 Models for the fractal dimension	3
1.2.1 Mean-field approximations	3
2 Morphological Transitions	7
2.1 Stochastic/energetic growth dynamics	7
2.1.1 BA/DLA-MF (λ -) model	7
2.1.2 BA/DLA-MF (p -) model	12
3 Unified Fractal Description	15
3.1 Theoretical model for the fractality	15
3.1.1 Solution to the ϵ - and p -transitions	17
3.1.2 Solution to the DBM transition	18
3.2 Order parameter and criticality	21
3.3 Universality	22
4 Outcome	27

Appendix A. Fractal dimensions of DLA and DBM	29
Appendix B. Models and methods	35
Appendix C. Additional preliminary results	39

Acknowledgements

In Spanish:

Principalmente agradezco a mis asesores, Dr. José Luis Carrillo Estrada y Dr. Víctor Dossetti Romero, por toda su confianza, paciencia y apoyo brindado durante el tiempo de mi formación doctoral.

Un agradecimiento también al comité de seguimiento de esta tesis, a la Dra. Minerva González Melchor, Dr. José Elías López Cruz y Dr. Emerson L. Sadurní Hernández, por sus observaciones y atención durante estos años.

Agradezco de manera especial a todo el personal administrativo, técnico y de apoyo del Instituto de Física, por su importante labor y gran ayuda.

Este trabajo de tesis fue realizado con el apoyo económico del Consejo Nacional de Ciencia y Tecnología de México.

Abstract

Stochastic growth processes give rise to diverse and intricate structures everywhere in nature, often referred to as fractals. In general, these complex structures reflect the non-trivial competition among the interactions that generate them. In particular, one of the most fundamental models to study these systems has been the paradigmatic Laplacian-growth model that exhibits a characteristic fractal to non-fractal morphological transition as the non-linear effects of its growth dynamics increase. So far, a complete scaling theory for this type of transitions, as well as a general analytical description for their fractal dimensions have been lacking. In this work, we show that despite the enormous variety of geometrical shapes, these morphological transitions have clear universal scaling characteristics. Using a fundamental particle-cluster aggregation models in two-dimensions, we introduce four non-trivial fractal to non-fractal transitions that capture all the main features of fractal growth. By performing the scaling analysis to the respective clusters and by constructing a dynamical model for their fractal dimension, we show that these morphological transitions are well described by a general dimensionality function regardless of their space symmetry-breaking mechanism, including the Laplacian case itself. Moreover, under the appropriate variable transformation this description is universal, i.e., independent of the transition dynamics, the initial cluster configuration, and the embedding Euclidean space.

Resumen

Los procesos de crecimiento estocástico dan origen a diversas e intrincadas estructuras por todas partes en la naturaleza, que comúnmente se les conoce como fractales. En general, estas complejas estructuras reflejan la competencia no trivial de las interacciones que las generan. En particular, uno de los modelos fundamentales usados para estudiar estos sistemas ha sido el paradigmático modelo de crecimiento Laplaciano, que exhibe una característica transición morfológica fractal/no-fractal al incrementar los efectos no-lineales de su dinámica de crecimiento. Hasta ahora, no se ha desarrollado una teoría completa de escalamiento para este tipo de transiciones, así como una descripción general analítica para dimensiones fractales. En este trabajo se muestra que, a pesar de la enorme variedad de formas geométricas, estas transiciones morfológicas tienen claras y universales características de escalamiento. Empleando modelos fundamentales de agregación partícula-cluster en dos dimensiones, presentamos cuatro transiciones no-triviales fractal/no-fractal que capturan las principales características de crecimiento fractal. Haciendo un análisis de escalamiento a los respectivos clusters y construyendo un modelo dinámico para su dimensión fractal, mostramos que estas transiciones morfológicas son bien descritas por una función general de dimensionalidad, sin importar el mecanismo de rompimiento de simetría involucrado, incluyendo el caso Laplaciano mismo. Más aún, bajo la transformación de variables adecuada, esta descripción es universal, esto es, independiente de la dinámica de transición, la configuración inicial y el espacio Euclídeo en las que existen.

Publications

The results of Chapters 2 and 3 have been subject to extensive peer-review processes and presented in the following publications.

The introduction of the interactive λ -model with its associated BA/DLA-MF morphological transitions, as well as our first example of controlled fractal growth, are presented in:

- “Fractality *á la carte*: a general particle aggregation model”, J. R. Nicolás-Carlock, J. L. Carrillo-Estrada, and V. Dossetti, *Scientific Reports* **6**, 19505 (2016).

The introduction of the p -model with its associated BA/DLA-MF morphological transitions, the derivation of the generalized dimensionality function $D(\Phi)$, and its application to the description of the fractality of the λ -, p -, and η - models, are presented in:

- “Universal fractality of morphological transitions in stochastic growth processes”, J. R. Nicolás-Carlock, J. L. Carrillo-Estrada, and V. Dossetti, *Scientific Reports* (2017) [In press].
- “Fractal to non-fractal morphological transitions in stochastic growth processes”, J. R. Nicolás-Carlock, V. Dossetti, and J. L. Carrillo-Estrada, in *Fractal Analysis - Applications in Health Sciences and Social Sciences* (ed. F. Brambila) Intech (2017) [In press].

The cover of the three previous publications is attached at the end of this work.

In addition, the derivation of the analytical solution to the fractality of the η -model of Chapter 3 is presented in:

- “The fractal dimensions of Laplacian growth: an information entropy approach to self-similar cluster characterization”, J. R. Nicolás-Carlock and J. L. Carrillo-Estrada [To be submitted].

A copy of the full manuscript is attached at the end of this work.

Introduction

“Clouds are not spheres, mountains are not cones, coastlines are not circles, and bark is not smooth, nor does lightning travel in a straight line. More generally, many patterns are so irregular and fragmented, that, Nature exhibits not simply a higher degree but an altogether different level of complexity.”

– Benoit B. Mandelbrot

In nature, fractal structures emerge in a wide variety of systems as an optimization of specific growth processes characterized by non-trivial self-organizing and self-assembling processes of pattern formation, restricted to the entropic and energetic conditions of their environment [1, 2, 3, 4]. Even more, the fractality of these systems determines many of their physical, chemical and/or biological properties, then, to comprehend the mechanisms that originate it, is very important in many areas of science and technology. One striking feature of these systems are the morphological transitions that they undergo as a result of the interplay of the entropic and energetic aspects of their growth dynamics that ultimately manifest in the geometry of their structure [5]. It is here where, despite their complexity, great insight can be obtained into the fundamental elements of their dynamics from the powerful concepts of fractal geometry [6, 7]. Such is the case of the Laplacian growth or Dielectric Breakdown Model (DBM) [8, 9], that has been the model of reference to study these systems, with important contributions to our understanding of far-from-equilibrium growth phenomena, to such extent that seemingly unrelated patterns found in nature, such as river networks or bacterial colonies, are understood in terms of a single framework of complex growth [10, 11]. However, a complete scaling theory of growth far-from-equilibrium has been missing and consequently, a comprehensive description of the fractality of systems that exhibit fractal to non-fractal morphological transitions is missing as well [7, 12].

One the most successful approaches used to tackle this problem has been the use of

stochastic growth models of particle aggregation. In general, aggregation phenomena are out-of-equilibrium processes of fractal pattern formation that are ubiquitous in nature [3], and since the introduction of the diffusion-limited aggregation (DLA) and ballistic aggregation (BA) models, a plethora of studies have been developed trying to understand the ultimate aspects of the aggregation dynamics that give rise to *self-similar* or fractal clusters, the relationship of this *fractality* with their physical and chemical properties, and the most effective methods and techniques to control fractal growth. In this work, in order to clarify important aspects of the theory of fractal to non-fractal morphological transitions and by following this statistical approach to fundamental particle-cluster aggregation dynamics, we present a general theoretical model for the scaling or fractality of these systems. As the main result, we show that regardless of their space symmetry-breaking mechanism, initial configuration and Euclidean embedding space, these morphological transitions are well described by a universal dimensionality function, including the Laplacian one. The presentation of these results is made as follows:

In *Chapter 1*, we present the fundamental models of fractal growth used: the DLA, BA and mean-field (MF) aggregation models, as well as the DBM as the first full morphological transition within the context of Laplacian growth. This includes, an account of the numerical and theoretical results reported over the years for the fractal dimension of the DLA and DBM in two and higher dimensions. In *Chapter 2*, by identifying the basic dynamical elements that drive fractal growth and under two modelling schemes, we introduce four two-dimensional non-trivial fractal to non-fractal transitions that are able to reproduce all the main morphologies observed in the literature. These transitions go from initial DLA or BA clusters towards linear structures characteristic of the MF model as function of one control parameter. For each of these, the scaling of the clusters is measured for different values of their control parameters using two standard methods: the two-point density correlation function and the radius of gyration. In *Chapter 3*, we introduce a general dimensionality equation that is able to describe the measured fractal dimensions and scaling of clusters generated from the previous models, including the DBM. This equation unifies the description of these transitions by allowing their classification using a single and characteristic parameter. Furthermore, it clarifies important aspects of nature of this transitions, such as their criticality, and most remarkably, it shows that the set of fractal dimensions that characterize each transition collapse into a single universal curve, independently of the growth process, initial cluster configuration, and embedding Euclidean space. Finally, in *Chapter 4*, we present a summary of the results of this work.

Chapter 1

Fractal Growth Models

1.1 Stochastic growth

The diversity of fractal morphologies in nature is just matched by the enormous amount of out-of-equilibrium processes that generate them, making the issue of establishing a unified and comprehensive theory of fractal growth a great challenge [2, 5, 6, 7]. However, it often happens that a simple model comes to unify diverse phenomena that once seemed to be completely unrelated. Such is the case of the Laplacian growth theory and its emblematic dielectric breakdown model (DBM), a paradigm of out-of-equilibrium growth that, due to its diversity of fractal morphologies, has received significant attention in diverse scientific and technological fields, from the oil industry, through bacterial growth, to even cosmology [10, 11, 12], with relevant applications in current neuroscience and cancer research [36, 37, 39]. Therefore, a precise characterization of this fundamental model in terms of its fractality is of the utmost importance.

1.1.1 DLA and BA models

In a generic growth process, the volume and surface of a given structure embedded in a Euclidean space of dimension d , can be described in terms of simple power-laws, $V \propto r^D$ and $dV/dr \propto r^\alpha$ respectively, where r is a characteristic radius, and D is the scaling or fractal dimension, with co-dimension $\alpha = D - 1$. In the Laplacian theory, the growth probability at a given point in space, μ , is given by the spatial variation of a scalar field, ϕ , i.e., $\mu \propto |\nabla\phi|$, where this scalar field is associated to the energy landscape of the growing surface of the cluster.

An example of such processes is the paradigmatic DLA model, where particles randomly aggregate one-by-one to a seed particle to form a cluster [10, 11, 12] (see Fig. 1.1). It has been found that the structure that emerges from this process exhibits

self-similar properties described by a D only dependent on the Euclidean dimension, d , of its embedding space [75, 76]. This issue has been the subject of extensive research, not only for the well-known two-dimensional case, where $D = 1.71$ (from numerical [45, 46, 47, 17, 48] and theoretical [56, 57, 59, 60, 62] results, see also Tables 1 and 2 in Appendix A), but in higher dimensions as well (although simulations [64, 65, 66, 67] and theory [68, 69, 70, 71, 72, 73, 74] are not in the best agreement, see Table 3 in Appendix A).

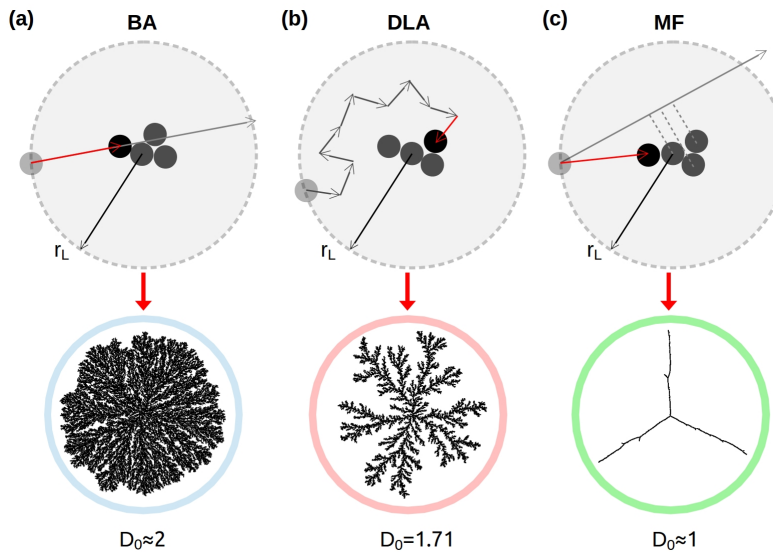


Figure 1.1: Schematic diagram of the fundamental aggregation models (top row) used in this work, where particles, that are launched one-by-one into the system from r_L with uniform probability in position and direction, (a) follow straight-line trajectories before aggregation in BA, (b) perform a random walk in DLA, and (c) get radially attached to the closest particle in the cluster as a result of an infinite-range radial interaction in MF. The morphology of MF emerge solely from its long-range interaction, as opposed to the stochastic BA and DLA. The corresponding characteristic cluster with its fractal dimension D_0 are shown in the bottom row.

Furthermore, when it was found that D is highly dependent on the mean square displacement of the particles' trajectories before aggregation, the theory has been extended to consider a more general and interesting growth process [13, 14, 15, 16, 17] in which the mean-square displacement of the particles' trajectories, as a control parameter, generates a continuous morphological transition that can be neatly described through the fractal dimension of the walkers' trajectories, d_w . This transition goes from a compact cluster with $D = d$ for $d_w = 1$, as expected for BA dynamics, to

the DLA fractal for $d_w = 2$ [18]; see Fig. 1.1. This BA-DLA transition has been reproduced in diverse and equivalent aggregation schemes, e.g., of wandering particles under drift [13], or with variable random-walk step size [14], by imposing directional correlations [15, 16], and through probabilistically mixed aggregation dynamics [17].

1.1.2 Mean-Field (MF) aggregation model

On the opposite side of the DLA and BA models (which can be regarded as pure-stochastic aggregation models), there is an immediate extension that incorporates the effects of long-range attractive interactions. This is the mean-field aggregation model, where particles aggregate to the closest particle in the cluster as soon as they enter into the system in response to an infinite or system-size attractive interaction (see Fig. 1.1).

1.1.3 Dielectric Breakdown Model (DBM)

However, one of the most challenging aspects of the theory arises when the growth is not purely limited by diffusion, e.g., when it takes place under the presence of long-range attractive interactions, where strong screening and anisotropic effects must be taken into account. In this case, the growth probability has been generalized to the form $\mu \propto |\nabla(\phi)|^\eta$, where $\eta \geq 0$ is the growth probability parameter, a real number associated to the net effect of all non-linear interactions [8, 24, 9, 26, 20, 21, 25, 40, 41, 42] (see Fig. 2). For a given embedding Euclidean space of dimension d , this process generates a characteristic morphological transition as a function of η , that goes from an initial compact structure with $D = d$ for $\eta = 0$, associated with Eden clusters, passing through DLA fractals for $\eta = 1$, to a linear cluster with $D = 1$ as $\eta \rightarrow \infty$. In addition, it has been suggested that the transition to the last one occurs at a critical value $\eta \approx 4$, where this criticality is understood in terms of the fractality of the system, i.e., the value for η at which $D \approx 1$ [20, 21, 19]. Nonetheless, the use of the fractal dimension D as an order parameter, able to describe the criticality of these transitions, still needs some clarification.

1.2 Models for the fractal dimension

1.2.1 Mean-field approximations

Although with important limitations, the generalized Honda-Toyoki-Matsushita mean-field equation [75, 76, 23], is among the best analytical results to describe the fractality of these models. In the case of DLA where D , only depends on the Euclidean dimen-

sion, d , of its embedding space, $D(d)$ given by,

$$D(d) = \frac{d^2 + 1}{d + 1}. \quad (1.1)$$

For $d = 2$, this expression predicts $D = 5/3 \approx 1.67$, different from the widely reported and numerically obtained value for off-lattice DLA, $D = 1.71$.

For the BA-DLA morphological transition, D is related to the dimension of the walkers' trajectories, d_w , $D(d, d_w)$ is given by,

$$D(d, d_w) = \frac{d^2 + d_w - 1}{d + d_w - 1}. \quad (1.2)$$

Here, for $d_w = 1$ one gets $D = d$, as expected for ballistic-aggregation dynamics, whereas for $d_w = 2$, the value $D = 5/3$ for DLA is recovered.

Finally, in the most general scenario of the DBM, we have that,

$$D_{\text{MF}}(d, d_w, \eta) = \frac{d^2 + \eta(d_w - 1)}{d + \eta(d_w - 1)}. \quad (1.3)$$

For $d_w = 2$, it is intended to describe the DBM in any embedding dimension d . In particular, for the case $d = 2$, this expression provides a good qualitative description of the fractality of the DBM transition, however, due to its mean-field limitations, it fails to precisely reproduce the reported numerical results for $D(\eta)$ [26, 25]. For example, it underestimates the known fractal dimension of DLA clusters for $d = 2$, nor does it clearly predict any criticality as suggested. As far as we know, there is not any analytical result able to fully describe the scaling or fractality of these and similar processes [7, 12] (see Fig. 3 and Table 4 in Appendix A).

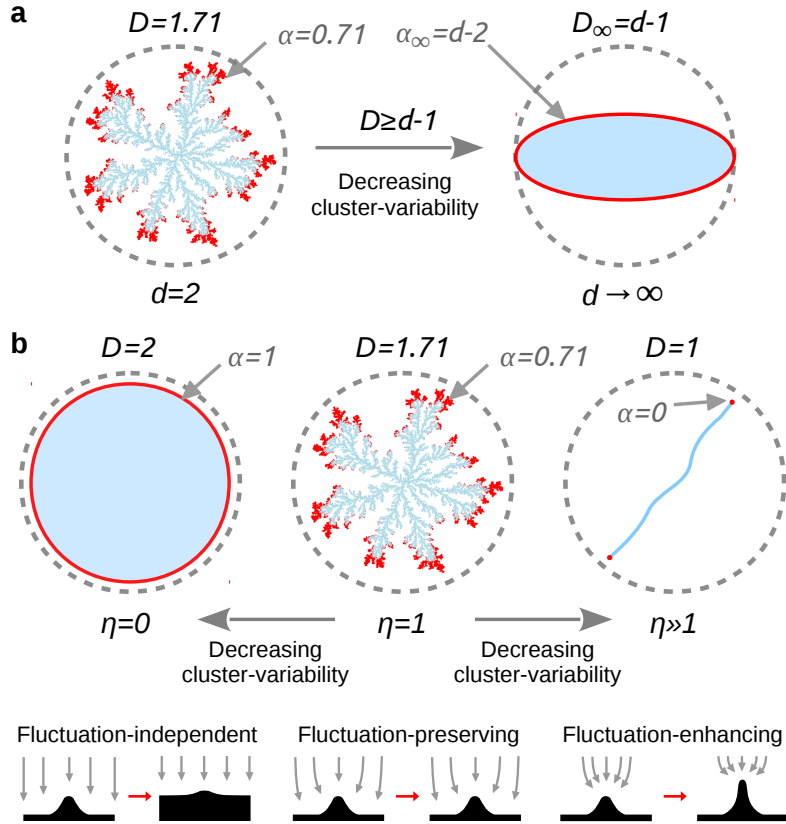


Figure 1.2: **The Laplacian framework.** (a) Characteristic morphological and scaling features of the DLA fractal (with its cluster in blue and growing front in red), for $d = 2$ (left) and $d \rightarrow \infty$ (right) according to the Ball inequality, $D \geq d - 1$ [68]. (b) Characteristic features of the DBM for $d = 2$ and as a function of η (top), with a generic description of the corresponding growth dynamics (as related to σ) at a small portion of the growing front (bottom).

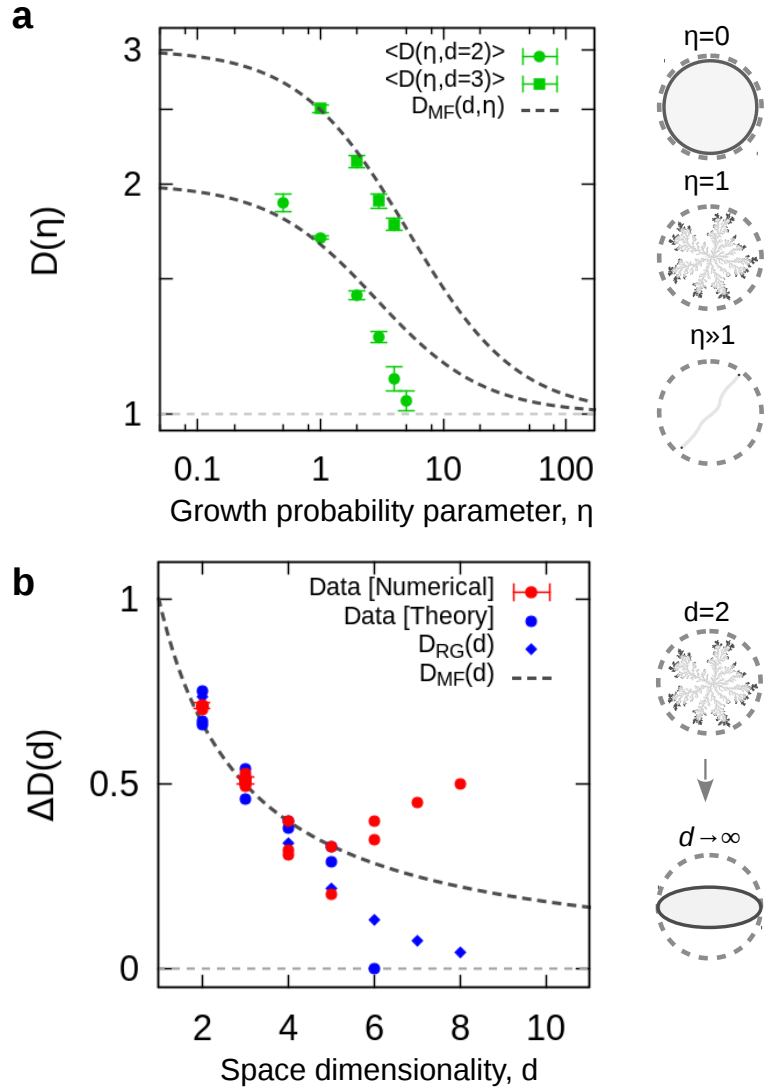


Figure 1.3: **DBM and DLA dimensions.** (a) Numerical results (Table 3 Appendix A) for $D(d, \eta)$ of the DBM for $d = 2$ and 3 in a log-log plot. (b) Numerical (red) and theoretical (blue) results (Table 4 Appendix A) for $D(d, \eta = 1)$, expressed through $\Delta D = D - (d - 1)$, of the DLA model.

Chapter 2

Morphological Transitions

2.1 Stochastic/energetic growth dynamics

The fundamental dynamical elements of aggregation that drive the fractal growth are mainly two: a stochastic one, coming from the particles' trajectories randomness, and an energetic one, coming from attractive interactions. With regard to the latter, there are two physical mechanisms related to these interactions and two models that are able to reproduce their effects. First, the model we will refer to as λ -model [27], incorporates the screening effects associated to long-range attractive interactions (such as those coming from an attractive radial potential) by means of an effective interaction radius λ , as illustrated in Fig. 2.1. Second, the model referred here to as the p -model [28], incorporates anisotropy effects coming from surface-tension-like interactions by means of a Monte Carlo approach to aggregation using fundamental stochastic and energetic models as explained bellow and illustrated in Fig. 2.1. Therefore, by controlling the interplay of any of these two mechanisms with a pure stochastic model (in this case the DLA or BA models), one is able to generate fractal to non-fractal morphological transitions.

There is an additional method to construct such morphological transitions that does not incorporates the energetic element, at least in an explicit manner. This method is based on the concept of penetration length and active growing front and, as the previously introduced models, it uses the BA and DLA models. However, this method will not be discussed here, nonetheless, some preliminary results are shown in Appendix C.

2.1.1 BA/DLA-MF (λ -) model

In the first approach to morphological transitions, we will consider the case when long-range attractive interactions are introduced in the growth dynamics. In this case, the

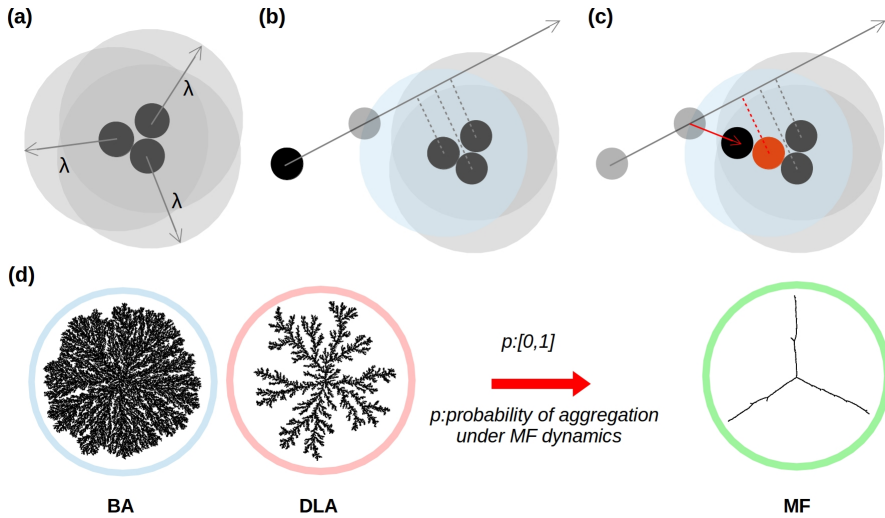


Figure 2.1: Schematic diagrams of the *energetic* aggregation schemes. For the λ -model: (a) every particle in the cluster is provided with an effective radius of aggregation λ . (b) A particle “collides” with the cluster when its trajectory intersects for the first time the interaction boundary of any aggregated particle. (c) The particle is aggregated to the closest particle along its direction of motion. This is determined by the position of the aggregated particles projected onto the direction of motion of the incoming particle. For the p -model: (d) a Monte Carlo approach to aggregation is established through the variable $p \in [0, 1]$, that controls the probability of aggregation under MF dynamics.

way to obtain self-similar clusters, that is, clusters with a single fractal dimension, is to maintain a proper balance between the energetic and entropic contributions to the growth process. This can be done by considering an aggregation radius, λ , associated with the range of the interaction for each particle in the growing cluster.

For example, for $\lambda = 1$, or *direct-contact* interaction, the usual DLA or BA models are recovered, see Figs. 2.2 and 2.3. When $\lambda > 1$, the attractive interactions modify the local morphology of the aggregates, leading to a more stringy structure. Two well defined features emerge due to the interplay of the long-range interactions and the way particles approach the cluster (in relation to their trajectories): a *multiscaling* branching growth and a crossover in fractality, from $D \rightarrow 1$ (as $\lambda \rightarrow \infty$) to $D = D_0$ (when $N \rightarrow \infty$).

It can be appreciated that this growth presents three well defined stages. In the first one, the growth is limited by the interactions and is characterized by $D \rightarrow 1$ as

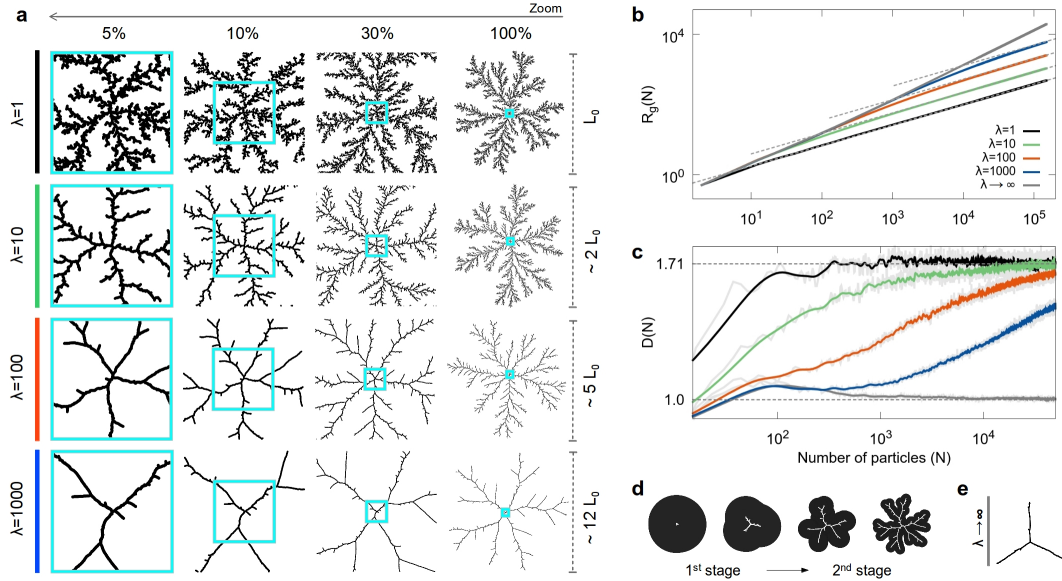


Figure 2.2: (a) Multiscaling aggregates based on DLA, containing $N = 150 \times 10^3$ particles each, for $\lambda = 1, 10, 100$ and 1000 units, visualized at 5% , 10% , 30% and 100% of their total size. The blue squares display the multiscaling evolution of the structure. (b) Radius of gyration, R_g , and (c) fractal dimension, D , versus the number of aggregated particles, N , in log-log and lin-log plots, respectively. Notice that, when $\lambda \rightarrow \infty$, the structure of the aggregates tends to MF ($D = 1$). (d) Evolution of the growing front for the first two stages of growth. (e) Typical structure of a MF aggregate.

$\lambda \rightarrow \infty$. This is due to the fact that the radial size of the cluster is small compared to λ . In consequence, the individual interaction regions of the aggregated particles are highly overlapped, forming an almost circular envelope or effective boundary of aggregation around the cluster. This makes the last aggregated particles the most probable aggregation point in the cluster for the next incoming particle. Because of this, there is a tendency for the clusters to develop three main arms or branches, clearly seen as $\lambda \rightarrow \infty$. This structural feature is reminiscent of a mean-field (MF) behavior. In the second stage, clusters exhibit a transition in growth dynamics. Here, the envelope starts to develop small deviations from its initial circular form, with typically three main elongations or growth instabilities associated with the main branches. When the distance between the tips of two adjacent branches becomes of the order of λ , a bifurcation process begins, generating multiscaling growth. Then, when the interactive envelope develops a branched structure itself, particles are able to penetrate

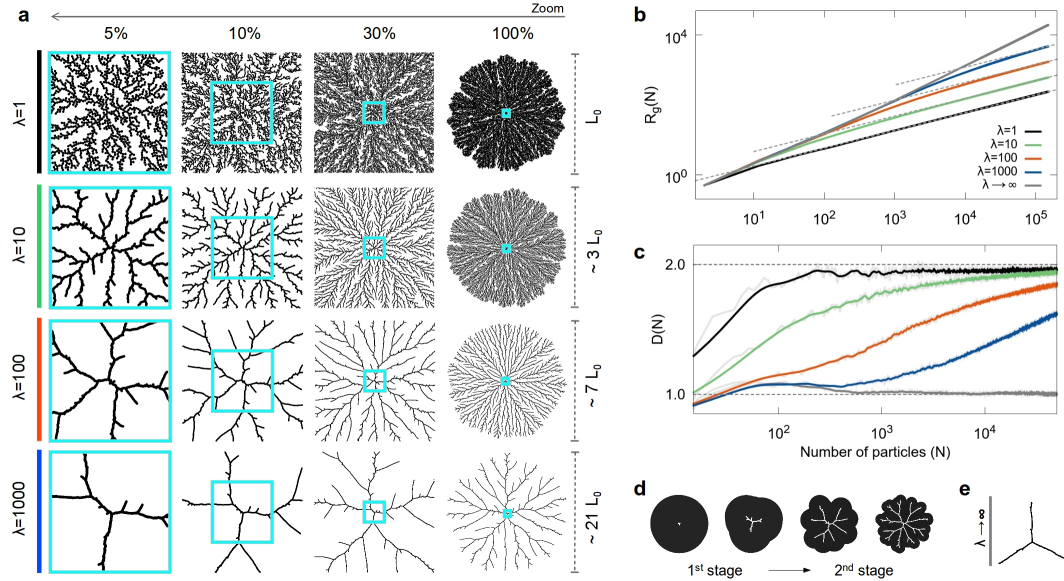


Figure 2.3: (a) Multiscaling aggregates based on BA, containing $N = 300 \times 10^3$ particles each, for $\lambda = 1, 10, 100$ and 1000 units, visualized at 5% , 10% , 30% and 100% of their total size. (b) Radius of gyration, R_g , and (c) fractal dimension, D , versus the number of aggregated particles, N , in log-log and lin-log plots, respectively. (d) Evolution of the growing front for the first two stages of growth. (e) Typical structure of a MF aggregate.

into the inner regions of the aggregate and another transition in growth dynamics takes place, from *interaction-limited* to *trajectory-limited*. In the third stage, when the distance among the tips of the main branches becomes much larger than λ , growth is limited by the mean squared displacement of the wandering particles. In this case, the asymptotic value $D = D_0$ and the main features in the global structure of the cluster are remarkably recovered as $N \rightarrow \infty$, inheriting the main characteristics of the entropic aggregation-model used, either DLA or BA. That is, even though interactions leave a strong imprint in the local structure and fractality of the clusters, the stochastic nature of the particle trajectories will ultimately determine their global characteristics.

However, taking into account that the spatial size of the clusters is proportional to the radius of gyration $R_g \propto N^{1/D}$, the desired balance between entropic and energetic forces — the latter related to the long-range attractive interaction and to the parameter λ — can be achieved by scaling the interaction range itself with the number of particles in the cluster through $\lambda(N) = \lambda_0 N^\varepsilon$, where λ_0 is fixed to one, while ε is the scaling parameter that takes values in $[0, 1]$; we will refer to ε as the *branching*

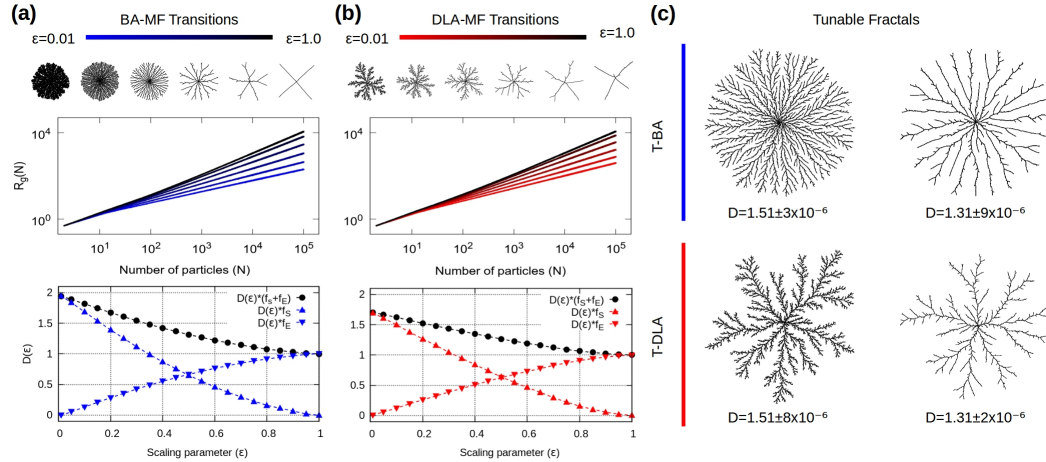


Figure 2.4: In (a) and (b), aggregates grown with specific values of ε in the interval $[0.01, 1]$ with the λ -model (top row) and log-log plots for R_g (middle row) for (a) BA and (b) DLA with $N = 10^5$ particles. One can appreciate the difference in the morphology of these monofractal-aggregates with respect to ε . Additionally, the specific entropic and energetic contributions to the clusters fractal dimension $D(\varepsilon)$ are shown in the bottom panes. (c) Clusters based in BA (left) and DLA (right) with the same fractal dimension, from top to bottom $D = 1.51$ and 1.31 , grown with a very high precision around the desired value.

parameter. Given a fixed value of ε and this choice for $\lambda(N)$, every aggregate grown under these conditions has a precise and uniquely defined fractal dimension $D = D(\varepsilon)$. In fact, using $D(\varepsilon)$ for different values of ε , one can define the entropic and energetic ratios given by $f_S = (D(\varepsilon) - 1)/(D_0 - 1)$ and $f_E = 1 - f_S$, respectively, that quantify the specific entropic and energetic contribution to the fractal dimension of the clusters (see Fig. 2.4). Here, one can clearly appreciate the transition in growth regimes from entropic, when $\varepsilon \rightarrow 0$, to energetic, as $\varepsilon \rightarrow 1$, and the non-trivial interplay between them to generate each cluster with a specific dimensionality.

Additionally, this model allows one to estimate $\varepsilon(D)$, in order to grow aggregates with any prescribed fractal dimension D in $[1, D_0]$, once the underlying entropic model, DLA or BA, is selected. As such, we are no longer restricted to the purely entropic models of fractal growth with a constant λ , as the energetic contribution of the long-range attractive interactions is maintained through the varying $\lambda(N)$, enabling one to explore in a continuous manner the full range of clusters with fractal dimensions in $[1, D_0]$. Nonetheless, the purely entropic contribution of the underlying models (DLA or BA) have two important contributions to the clusters' structure: first, they

establish an upper limit to the fractal dimensionality (D_0), and second, they define a characteristic morphology to the clusters (that of DLA or BA). This kind of control over the clusters' fractal dimension and the range it spans, as well as over the morphology of the clusters, has not been obtained before under any other related scheme of fractality tuning [27].

2.1.2 BA/DLA-MF (p -) model

In the second approach, a general stochastic aggregation process can be modelled under a Monte Carlo scheme involving three fundamental and simple *off-lattice* models of particle-cluster aggregation. On the one hand, the well-known BA and DLA models provide disordered/fractal structures through their stochastic (entropic) dynamics. On the other, we introduce a mean-field (MF) model of long-range interactive particle-cluster aggregation [27, 28], that provides the most energetic (and noiseless) aggregation dynamics that, simultaneously, acts as the main source of anisotropy. Then, the statistical combination of these models results in off-lattice DLA-MF and BA-MF dynamics, whose morphological transitions can be controlled by the *mixing* parameter $p \in [0, 1]$, associated with the probability or fraction of particles aggregated under MF dynamics, $p = N_{\text{MF}}/N$, where N is total number of particles in the cluster. Therefore, as p varies from $p = 0$ to $p = 1$, it generates two non-trivial transitions from fractals (DLA) or fat fractals (BA) with fractal dimension $D = D_0$, to non-fractal clusters with $D = 1$ (MF), that capture all the main morphologies of fractal growth [6] (see Fig. 2.5).

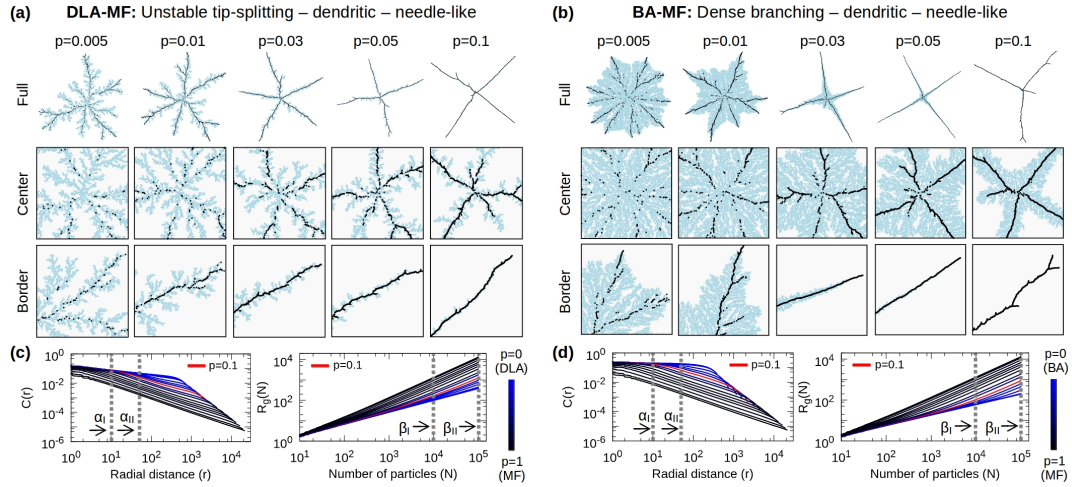


Figure 2.5: Clusters of 1.5×10^5 particles grown with the indicated values of p , are shown at different magnifications for the (a) DLA-MF and (b) BA-MF transitions. Particles aggregated under DLA/BA are coloured in light-blue while those through MF in black. These transitions exhibit fast morphological transformations as p increases, from unstable tip-splitting (DLA) or dense branching (BA), through (inhomogeneous) dendritic, to needle-like growth (MF). (c-d) $C(r)$ and $R_g(N)$ display deviations from a well-defined linear behaviour for different p , revealing the inhomogeneity or crossover effects in these clusters. This is better seen at low scales, where the stochasticity of DLA or BA dominate the local growth, whereas MF tends to dominate the global morphology as $p \rightarrow 1$. In both cases, the dynamical growth-regime changes at $p \approx 0.1$. Labels α_I , α_{II} , β_I and β_{II} indicate the scales used for the scaling analysis.

Chapter 3

Unified Fractal Description

3.1 Theoretical model for the fractality

Despite the complexity of the transitions mentioned above, a simple model can be established to describe their fractality or scaling. This is done by considering that the fundamental dynamical elements that drive the fractal growth are mainly two: *stochastic* and *energetic*. As previously discussed, when the growth dynamics is purely driven by stochastic processes, as in the case of DLA ($\eta = 1$) or BA (similar to $\eta = 0$), the resulting structure is either a fractal (DLA) or a compact fat-fractal (BA) with $D \leq d$. However, when an energetic element is introduced in the growth dynamics, the fractal dimension of the clusters decreases; for example, $D \rightarrow 1$ as $\eta \rightarrow \infty$ in the DBM.

As such, in the most general case, we consider that these transitions start with clusters produced by purely stochastic dynamics, with $D = D_0$, where D_0 stands for the fractal dimension of the clusters in this regime. Further on, as energetic mechanisms that drive spatial symmetry-breaking increase, such as strong non-linear interactions, for example, these clusters collapse to linear structures. Let us also consider that all the information regarding the effects of stochastic and energetic growth-dynamics is encoded in an effective control parameter Φ , allowing us to define a generalized dimensionality function $D(\Phi)$. In this way, as a function of Φ , we require that $D(\Phi) = D_0$ for $\Phi = 0$ and that $D(\Phi) \rightarrow 1$ as $\Phi \rightarrow \infty$ along the transition. In terms of the co-dimension, $\hat{D} = D - 1$, we would have $\hat{D}(\Phi) = D_0 - 1$ for $\Phi = 0$ and $\hat{D}(\Phi) \rightarrow 0$ as $\Phi \rightarrow \infty$, correspondingly. Additionally, for this kind of morphological transitions, it has been observed that the dependence of D on the control parameter is smooth and monotonically decreasing [21, 24, 26, 27, 30, 31]. From this, since $dD/d\Phi = d\hat{D}/d\Phi$ is satisfied, the most general solution for the scaling of the clusters is obtained from $d\hat{D}/d\Phi = -f(\hat{D})$. By expanding $f(\hat{D})$ as a Taylor series we have:

$d\hat{D}/d\Phi \approx -[f_0 + f_1\hat{D} + O(\hat{D}^2)] \approx -f_0 - f_1\hat{D}$. Here we have truncated the series up to the linear term as, again, we expect \hat{D} to vary smoothly along the transition. Thus, by integrating on both sides of the equation for a given and finite \hat{D} and Φ , i.e., $\int_{\hat{D}_0}^{\hat{D}} d\hat{D}'/(f_0 + f_1\hat{D}') = \int_0^\Phi d\Phi'$ and by taking into account the condition that $\hat{D}(\Phi) \rightarrow 0$ as $\Phi \rightarrow \infty$, we obtain for $D(\Phi)$:

$$D(\Phi) = 1 + (D_0 - 1)e^{-\Phi}, \quad (3.1)$$

where the constant f_1 has been absorbed in the control parameter Φ .

Under the conditions stated above, equation (3.1) is the most general form for the fractality of clusters found in morphological transitions, driven by stochastic and energetic mechanisms. For a particular case, the effective parameter Φ must still be found and is expected to depend on the parameters of a given system. As explained below, finding the correct Φ is not trivial and special dynamical conditions over D will be required. Before considering a more general scenario, let us now show why this equation is suitable to characterize these systems by considering the DBM mean-field equation first.

The mean-field result given in equation (1.3) belongs to a special case of the family of equations given in (3.1). Starting with the first-order approximation in Φ of equation (3.1), it follows that,

$$D^{(1)}(\Phi) = 1 + \frac{D_0 - 1}{1 + \Phi} = \frac{D_0 + \Phi}{1 + \Phi}. \quad (3.2)$$

Here, by setting $D_0 = d$ and from direct comparison with equation (1.3), one is able to observe that these expressions are equivalent, with Φ being nothing but $\Phi_{MF} = \eta(d_w - 1)/d$. This approximate result makes the relation between the effective parameter Φ and the actual parameter of the transition (in this case η) more evident and, for a given d (with $d_w = 2$), it exhibits a linear relation between the parameters, $\Phi \propto \eta$, which, as stated before, does not provide the correct solution to D due to its mean-field nature [26, 25]. Thus, a more general function for $\Phi(d, \eta)$ is still required.

There is one more condition that should be imposed over D in order to have a better and more general prescription for Φ . When the fractal dimension of a cluster goes from $D = D_0 \leq d$ to $D = 1$ throughout the transition, due to the competition of the stochastic and energetic elements of the growth dynamics, two regimes can be clearly defined in the extremes. For this to happen, there will necessarily exist a regime change in between, where neither the stochastic nor the energetic mechanisms dominate. Regarding the behavior of D , let us consider that this change in regime is associated with the point where the second derivative of D with respect to its control parameter becomes zero. This is, if $\Phi = \Phi(D_0, \zeta)$, where ζ is the parameter that controls the transition of a given system, then, there is an inflection point ζ_i that

satisfies, $d^2\hat{D}/d\zeta^2|_{\zeta=\zeta_i} = 0$. This *inflection* condition, from equations (3.1) and (3.2), translates to $[(d\Phi/d\zeta)^2 - d^2\Phi/d\zeta^2]|_{\zeta=\zeta_i} = 0$ and $[2(d\Phi/d\zeta)^2 - (1+\Phi)d^2\Phi/d\zeta^2]|_{\zeta=\zeta_i} = 0$.

For example, as it can be observed in the DBM mean-field case by identifying ζ as η , the relation between parameters is linear, i.e., $\Phi_{MF} = \Lambda\zeta/D_0$ (with $\Lambda = d_w - 1$ and fixed D_0), making it impossible to define ζ_i , as the inflection condition cannot be satisfied. Therefore, we propose $\Phi(D_0, \zeta) = \Lambda\zeta^\chi/D_0$ as a general *ansatz* for Φ , where Λ and χ are two positive real numbers that are associated with the strength of the screening/anisotropy-driven effective growth forces, to be determined either theoretically or phenomenologically according to the system under study. Then, from equation (3.1), the newly proposed form for the effective parameter $\Phi(D_0, \zeta)$ allows us to define a general dimensionality function $D(D_0, \zeta)$, characterized by an inflection point ζ_i , associated with a regime change in growth dynamics that satisfies $\Lambda\zeta_i^\chi/D_0 = (\chi - 1)/\chi$. Additionally, from equation (3.2), the inflection point for the first-order approximation $D^{(1)}(D_0, \zeta)$ is characterized by $\Lambda\zeta_i^\chi/D_0 = (\chi - 1)/(\chi + 1)$. In this way, the expressions for the generalized dimensionality function $D(D_0, \zeta)$ describe the scaling of the clusters along a continuous morphological transition from $D = D_0$ for $\Phi(\zeta) = 0$ towards $D = 1$ as $\Phi(\zeta) \rightarrow \infty$, with a well-defined regime change in growth dynamics at ζ_i . In the following, in order to test our model, we will apply it to two morphological transitions, namely DLA-MF and BA-MF, newly developed for this work. Then, we will address the DBM once more, aiming to develop a possible solution to its fractality. Finally, we will discuss the universal scaling presented by these systems.

3.1.1 Solution to the ϵ - and p -transitions

It is necessary to remark that the DLA-MF and BA-MF transitions in the p -model are characterized by inhomogeneous clusters, i.e., structures with non-constant scaling as shown in Figures 6c and 6d, in contrast with the ones present in BA-DLA [18, 16] and the DBM [8, 20] characterized by monofractals. These multiscaling features reveal a crossover behaviour that can be properly quantified by measuring a local or effective, $D(p)$, at different scales [7], as shown in Figure 7a (details for the values of the parameter used to produce Figure 7 are presented in Table 1). Analytically, all measurements can be described by equations (3.1) and (3.2), using Λ and χ as fitting parameters. Indeed, the data for $D(p)$ as obtained through the scaling analysis of $C(r)$, is very well described by equation (3.1), whereas equation (3.2) better describes the results obtained through $R_g(N)$. In the case of the λ -model, the BA/DLA-MF transitions are governed by the branching parameter, ε , which is equivalent to the mixing parameter p of the p -model. Nonetheless, in the λ -model, the clusters exhibit a monofractal behaviour all along the transition as measured by $R_g(N)$. Thus, the data obtained is then described by equation (3.1) as fitting function. This analysis is

presented in Fig. 3.1.

Table 3.1: Parameters for the plots of $D(p)$ and $D(q)$ in Figure 7. In the first block we present the parameter values used to describe $D(p, \Lambda, \chi)$, using equations (3.1) and (3.2). In the second block, description for the $D(q, \chi)$ data obtained through $C(r)$ and $R_g(N)$. In this prescription, χ is the only free parameter to be determined and, by construction, all the inflection points are located at $q = 1$. All of the fittings to the numerical data were performed using the *gnuplot* embedded algorithms.

Model	Transition	Method	Scale	Λ	χ	D_0	p_i, q_i
p	DLA-MF	$C(r)$	α_I	15.4	2.24	1.67	0.29
			α_{II}	71.5	1.82		0.08
		$R_g(N)$	β_I	33.8	1.41	1.71	0.03
			β_{II}	101.6	1.32		0.01
	BA-MF	$C(r)$	α_I	11.6	1.61	1.94	0.18
			α_{II}	45.4	1.38		0.04
		$R_g(N)$	β_I	124.8	1.95	1.95	0.06
			β_{II}	1547.7	2.05		0.02
λ	DLA-MF	$R_g(N)$	$10^3 - 10^5$	6.10	1.52	1.70	0.21
	BA-MF	$R_g(N)$	$10^3 - 10^5$	6.35	1.43	1.95	0.19
p	DLA-MF	$C(r)$	-	-	1.69	1.67	1.0
		$R_g(N)$	-	-	1.34	1.71	1.0
	BA-MF	$C(r)$	-	-	1.39	1.94	1.0
		$R_g(N)$	-	-	1.88	1.95	1.0
λ	DLA-MF	$R_g(N)$	-	-	1.52	1.70	1.0
	BA-MF	$R_g(N)$	-	-	1.43	1.95	1.0

3.1.2 Solution to the DBM transition

At this point in the analysis, it is important to consider the two-dimensional DBM transition as well. As previously discussed, within the mean-field approximation, we have that equation (3.2), with $\Phi_{MF} = \eta/d$ ($d_w = 2$), fails to precisely describe the fractality of the transition (see Fig. 3.2a). However, by means of equation (3.1) and the general *ansatz*, $\Phi(D_0, \eta) = \Lambda\eta^\chi/D_0$, with $D_0 = d$, a better agreement with the data is achieved. The parameters Λ and χ can be obtained by fitting our model to the data as before (dashed black curve in Fig. 3.2a), nonetheless, here we also show how they can be analytically calculated. Setting $d = 2$, the first parameter Λ can be obtained by using the well known result for the two-dimensional scaling of DLA, $D = 1.71$, that is associated with $\eta = 1$ for the DBM. From equation (3.1), this leads to $\Lambda = -d \log((D_{\eta=1} - 1)/(d - 1)) = -2 \log(0.71) \approx 0.685$. Then, the χ parameter is obtained from the dynamical condition imposed over D , given by $\Lambda\eta_i^\chi/d = (\chi - 1)/\chi$. Considering that the DLA fractal ($\eta = 1$) can be associated to a particular (possibly

critical [30, 31]) dynamical state, that defines the regime change of the DBM transition, from non-fractal ($D_0 = d$, $\eta = 0$), through fractal (DLA, $\eta = 1$), to non-fractal ($D = 1$, $\eta \gg 1$), then we can set $\eta_i = 1$, leading to $\chi = 1/(1 - \Lambda/d) \approx 1.52$. As it can be appreciated in Fig. 3.2 (solid black curves), this analytical result agrees very well with the data for $D(\eta)$ within a self-contained framework, provided that the DLA state marks the point of change in regime (see also Table 4 in Appendix A). For the rest of this work, we will consider $\eta_i = 1$ as the transitional point for the DBM.

Particularly, a good insight into this solution can be found within the context of information theory as applied to out-of-equilibrium growth, where special attention has been given to the entropy production rate of growing clusters as function of their active front [30, 31], that in addition, is supported by the fundamental Turkevich-Scher conjecture, $D = 1 + \alpha^*$, that relates the fractal dimension of the cluster to the dimension of the most active region of its growing front, $\alpha^* = \alpha$, indicating that the scaling of the active perimeter, i.e, the co-dimension, contains the information needed to uniquely define the fractality of the cluster itself [69, 12]. A measure of this information, and the connection to entropy production, is found under the formalism of multifractal sets, where the information entropy, S , is related to the generalized dimension, D_q , through the first-order moment of the generalized Rényi entropies, $S_q = \log \sum_{i=1}^n p_i(\epsilon)^q / (q-1)$, as, $D_{q=1} = \lim_{\epsilon \rightarrow 0} S_{q=1} / \log \epsilon$, where $S_{q=1} = -\sum_{i=1}^n p_i(\epsilon) \log p_i(\epsilon)$, and $p_i(\epsilon)$ is the probability of a given growth event at a spatial observation scale, ϵ [56]. In the case of self-similar structures, such as those characterizing the full DBM transition, the generalized dimension becomes independent of q , making all the fractal dimensions D_q (such as, box-counting $q = 0$, information $q = 1$, or correlation $q = 2$) equivalent and directly proportional to the information entropy, leading to $S(d, \eta) = kD(d, \eta) = k + k\alpha(d, \eta)$, with $k = \log \epsilon$. In terms of the entropy production, this relation implies that, for a fixed observation scale, $\partial S / \partial \eta = k \partial \alpha / \partial \eta \rightarrow 0$, for either $\eta \rightarrow 0$ or $\eta \gg 1$. In other words, the amount of information needed to characterize the active perimeter of a compact circular cluster as $\eta \rightarrow 0$, or the active tip of linear structures as $\eta \gg 1$, does not grow as much as the one needed to characterize the intermediate fractal perimeter of clusters at $\eta \sim 1$ (see Fig. 1.2).

As previously shown for $d = 2$, the specific values for the Λ and χ parameters can be found numerically, via a fit to available data. Also, if the inflection condition is satisfied at $\eta = 1$ (the DLA point), the value of Λ for given d defines the value of $\chi = 1/(1 - \Lambda/d)$, and again, if data is available the value of Λ can be computed using Eq. (3.1) evaluated at $\eta = 1$. However, without prior knowledge of the DLA dimensions, here we show one way to find an analytical solution to $\Lambda(d)$.

The only analytical solution to $\Phi(d)$ known so far, is that of the mean-field description, $\Phi_{MF} = 1/d$, this is $\Lambda_{MF} = 1$. In general, $\Lambda(d)$ is expected to display a non-trivial behaviour as shown in Fig. 3.3a, where from Eq. (3.1), we applied $\Lambda[D(d)] = -d \log[(D(d) - 1)/(d - 1)]$, to all the available numerical results for $D(d)$

(Table 3 in Appendix A). In particular, we found that one way to construct this general $\Lambda(d)$ is by extending previous real-space renormalization-group (RG) results for on-lattice DLA [73, 74], to be valid in the continuous space. Under this RG approach, $D(k, d)_{RG} = 1 + \alpha(k, d) = 1 + \log \mu(k, d) / \log 2$, with,

$$\mu(k, d) = 1 + 2 \binom{d-1}{1} \phi_1 + \sum_{k=2}^{d-1} \binom{d-1}{k} \phi_k, \quad (3.3)$$

where, $\phi_k(d)$ are the growth potentials for a given lattice, and $\mu(k, d)$ is inversely proportional to the maximum growth probability, $p(d)_{max} = \mu(k, d)^{-1} = 2^{-\alpha(k, d)}$.

One of the shortcomings of this model is its heavy dependence on a lattice, that makes it overestimate the well-known DLA dimension for $d = 2$, for example, it predicts $D_{RG} = 1.737$ for a square lattice. Nonetheless, by construction, it is able to provide a lower boundary to $\Lambda(d)$. In the $d \rightarrow \infty$ limit, $\phi_k \rightarrow 1/2$, leading to $\mu(d)_\infty = 2^{d-1} + d/2$, that establishes the lower boundary, $\Lambda^- = -d \log[\log \mu(d)_\infty / \log(2^{d-1})]$. An upper boundary can still be established from the Ball inequality, where $D \geq d - 1$, must be always satisfied, leading to, $\Lambda^+ = -d \log[(d-2)/(d-1)]$. Thus, a solution for $\Lambda(d)$ must be such that the inequality, $\Lambda^- \leq \Lambda(d) \leq \Lambda^+$, where the equality will hold for $d \rightarrow \infty$, should always be satisfied (see Fig. 3.3b). Under the previous considerations, the extension to continuous space, i.e., $\mu(k, d) \rightarrow \mu(d)$, is done by observing that when $d \rightarrow \infty$, all the information in $\mu(d)$ regarding $D(d \rightarrow 2)$ is lost, as seen through Λ^- . Then, without loss of generality, this information can be recovered by taking $\phi_k = 1/2$ (the limit-value of ϕ_k as $d \rightarrow \infty$) starting from $k \geq 2$. This leads to,

$$\mu(d) = 1 - d/2 + 2^{d-2} + 2(d-1)\phi(d), \quad (3.4)$$

where $\phi_1 \rightarrow \phi(d)$, is a continuous function of d . Now, as $d \rightarrow 2$, we have that $\phi(d) = (2^{D(d \rightarrow 2)-1} - 1)/2$, and $\mu(d) = 1 + 2\phi(d) = 2^{D(d \rightarrow 2)-1}$. These forms for $\phi(d)$ and $\mu(d)$, suggest that D can be approximated as, $D(d) - 1 \approx (d-1)/\sqrt{2}$, as $d \rightarrow 2$. Therefore, we propose the following ansatz for $\phi(d)$,

$$\phi(d) = (2^{\sqrt{(d-1)/2}} - 1)/d, \quad (3.5)$$

that along with $\mu(d)$, provides,

$$\Lambda(d) = -d \log[\log \mu(d) / \log 2^{d-1}], \quad (3.6)$$

and consequently, the solution for $\Phi(d)$, see Fig. 3.3b. This solution satisfies the most rigorous restrictions imposed by the theory, and in particular, it predicts $D = 1 + 1/\sqrt{2} \approx 1.707$ for $d = 2$, in excellent agreement with the highly reported scaling of DLA. The complete solutions for $D(d, \eta)$ in $d = 2$ and $d = 3$, as well as $D(d)$ are shown in Figs. 3.3c and 3.3d, respectively.

3.2 Order parameter and criticality

Another important issue to consider here is that of the criticality of these morphological transitions, as well as its characterization using the fractal dimension as an order parameter, as previously suggested for the DBM [21]. In order to address this point in a comprehensive approach, let us first define a possible and suitable order parameter for these systems. This is done by plotting all of the data for $D(q)$ now as function of Φ itself, i.e., $D(\Phi)$, depicted in Figs. 3.1c and 3.2c. Notice that, in this description, the DLA/BA-MF (Fig. 3.1c) and DBM (Fig. 3.2c) transitions, starting from D_0 , approach the highly anisotropic regime ($D \approx 1$) in an almost identical manner, in excellent agreement with equations (3.1) and (3.2). Further on, in order to remove the dependence on D_0 , we introduce the reduced co-dimension, $D^* \in [0, 1]$, defined by $D^* = (D - 1)/(D_0 - 1)$, as the new “order parameter” of the system. From equations (3.1) and (3.2), we have,

$$D^*(\Phi) = e^{-\Phi}, \quad D^{*(1)}(\Phi) = \frac{1}{1 + \Phi}, \quad (3.7)$$

respectively. In this manner, under the new framework based on the co-dimension D^* , all the numerical results collapse into the universal curves given by equations (3.7) as can be appreciated in Fig. 3.4. These curves go from $D^* = 1$ for $D = D_0$, to $D^* \rightarrow 0$ for $D \rightarrow 1$. Moreover, the co-dimension D^* is not necessarily describing a real “order-disorder” transition but, rather, an isotropic-anisotropic one. The subtlety lies at the initial cluster configuration. This is, even though all transitions collapse to a linear “ordered” structure, the initial cluster configuration can also be considered as ordered, such as in the case of the DBM (associated to compact Eden clusters), or disordered, as in the case of the BA/DLA-MF transitions (a fractal for DLA and a fat-fractal for BA). Nonetheless, in terms of their isotropy, or preferential growth features, all transitions start from an isotropic (such as Eden or BA) or isotropic on-average (such as DLA) clusters, to a highly anisotropic structure as the rotational-symmetry is broken. These results suggest that characterization based on a rotational or angular quantity, such as the angular correlation function, would provide more insights into the nature of these transitions. In this case, some preliminary results are shown in Appendix C.

Furthermore, given that in any case the solutions for D^* are smooth functions that tend to zero in a continuous manner, defining a specific point where D^* becomes exactly zero is not possible. This implies that, the previously suggested critical point for the DBM, i.e., the value for η where $D \approx 1$ [21], cannot be treated as “critical” from the point of view of a formal critical phase-transition theory [30, 31]. In fact, this won’t be possible for any of the transitions analyzed in this work. Nevertheless, what it is still possible is to define *transitional* points, Φ_t , that are different from

Table 3.2: Transitional points for which the reduced co-dimension $D^* \approx 0$ for the λ - and p -models studied in this work. The labels α and β indicate that these data were obtained through measurements of the fractal dimension using $C(r)$ and $R_g(N)$, respectively.

Model	Data	D_0	χ	$\Phi_t(\nu = 0.1)$	q_t	$\Phi_t(\nu = 0.05)$	q_t	$D(q = 1)$
p	BA-MF (α)	1.94	1.39	2.3	4.5	3.0	5.4	1.72
	DLA-MF (α)	1.67	1.69	2.3	2.8	3.0	3.2	1.46
	BA-MF (β)	1.95	1.88	9.0	6.0	19.0	9.0	1.73
	DLA-MF (β)	1.71	1.34	9.0	21.7	19.0	37.8	1.62
λ	BA-MF	1.95	1.43	2.3	4.2	3.0	5.0	1.70
	DLA-MF	1.71	1.52	2.3	3.5	3.0	4.2	1.50

the points where the growth-regime changes. For the transitional points, the highly screening/anisotropy effects are dominant over the morphology of the cluster, thus, they correspond to points at which $D = 1 + \epsilon$, with $\epsilon \ll 1$, is the tolerance or deviation from $D = 1$ (for technical details see Table 3.2).

3.3 Universality

The final and most important implication of the previous findings is that the DBM and BA/DLA-MF transitions, although completely different, can be treated as belonging to the same universality class. In order to make sense of this, we must recall that, in two-dimensions, the DBM (for $\eta = 1$) and viscous fingering phenomena are said to belong to the same universality class as that of DLA, based on the fact that they are all characterized by the same fractal dimension, $D = 1.71$ [12, 33]. Therefore, by extending this idea to a whole set of dimensions, the *universality* of these morphological transitions must be understood in the sense that they are all described by the same set of fractal dimensions. Quite remarkably, under the description provided by the co-dimension $D^*(\Phi)$, the DBM and BA/DLA-MF morphological transitions belong to the same universality class which, in turn, implies that their mathematical description is independent of their spatial symmetry-breaking dynamics and initial configuration, therefore, these transitions will be described by the same curves in any embedding Euclidean dimension (see Fig. 3.4).

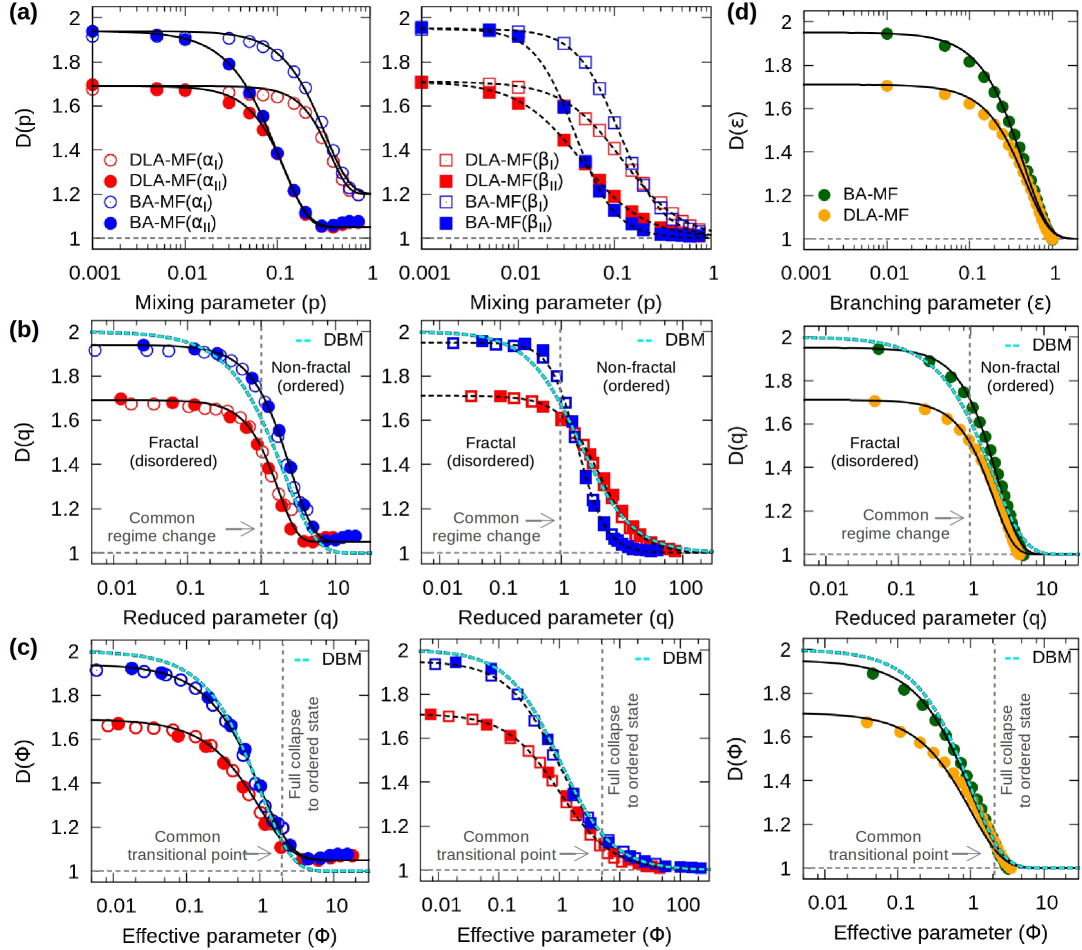


Figure 3.1: Scaling analysis for the p -model: (a) Plots of $D(p)$ for the DLA-MF and BA-MF transitions obtained from $C(r)$ (left), at small (α_I) and large (α_{II}) scales, and $R_g(N)$ (right), at medium (β_I) and large (β_{II}) scales, in correspondence to Fig. 2.5. These results are described by the solid and dotted curves given by equations (3.1) and (3.2), respectively, for different values of the parameters Λ and χ . (b) By plotting D as a function of $q = p/p_i$ (where p_i is calculated for each curve), data collapses into single master curves, $D(q)$. Note the common point of regime change at $q_i = 1$, marked with the vertical dashed lines. (c) In the description with the function $D(\Phi)$, all of the morphological transitions approach common transitional points where clusters have fully collapsed to an ordered structure, independently of the stochastic model used. (d) The corresponding scaling analysis is performed for the BA- and DLA-MF transitions obtained by using the λ -model. In this case, equation (3.1) was used. For further details about the parameter values used, see Table 3.1.

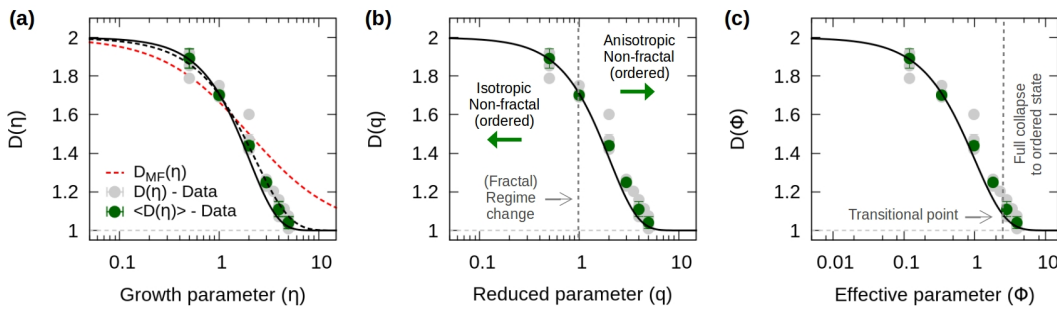


Figure 3.2: Scaling analysis for the DBM. (a) Plot of the fractal dimensions D as a function of η for the two-dimensional DBM transition (see Table 4 in Appendix A). Here, the failure of the mean-field description is evident (dashed red curve). A better agreement is obtained using equation (3.1), with $\Phi(D_0, \eta) = \Lambda \eta^\chi / D_0$, where $D_0 = 2$. By fitting the data with this equation, one obtains $\Lambda \approx 0.70$ and $\chi \approx 1.26$ with $\eta_i \approx 0.66$ (dashed black curve), while from the analytical analysis and by considering $\eta_i = 1$, $\Lambda = -2 \log(0.71) \approx 0.685$ and $\chi = 1/(1 - \Lambda/D_0) \approx 1.52$ (solid black curve). (b) Maintaining $\eta_i = 1$ as the transitional point, the analytical solution for $D(q)$ is equivalent to that for $D(\eta)$. (c) As well, from the analytical expressions, one can obtain the curve $D(\Phi)$.

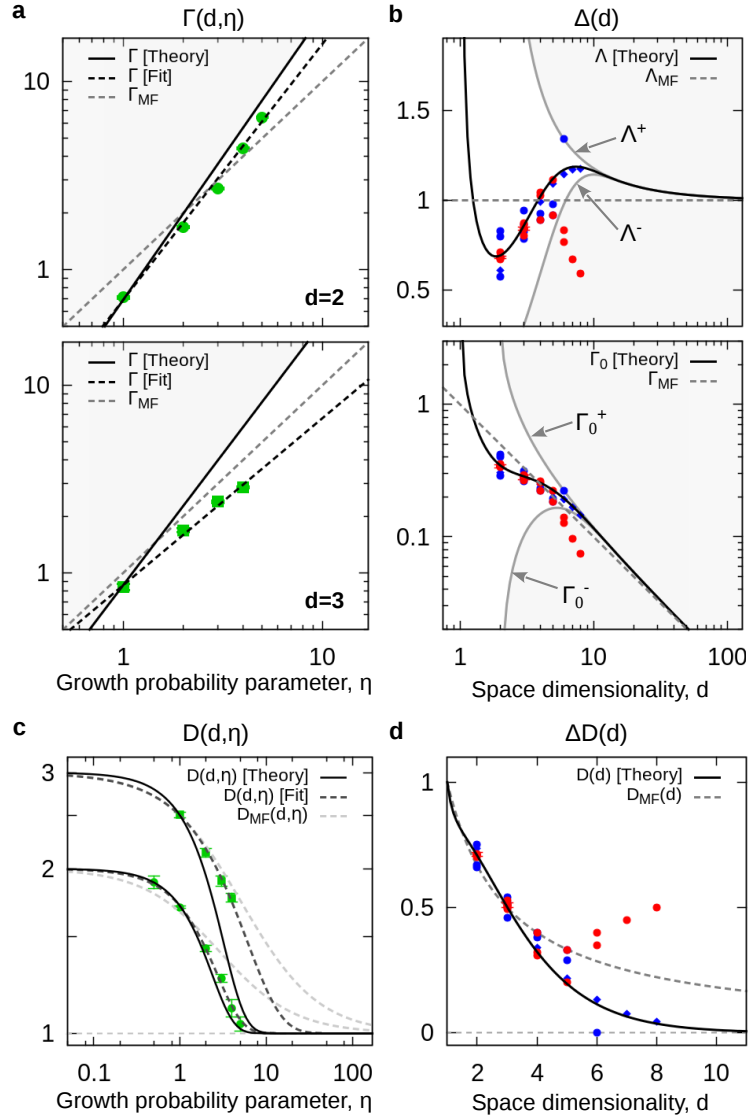


Figure 3.3: DBM and DLA solutions. In this figure, notice the change in notation $\Gamma = \Phi$. (a) Analysis of $\Gamma(d, \eta)$ in log-log plots for $d = 2$ (top) and $d = 3$ (bottom), using the data coming from Table 4 (Appendix A). Using Eq. (??) with $d = 2$, $\Lambda = 0.69$ with $\chi = 1.36 \pm 0.02$ from linear fit, and $\chi = 1.52$ from theory; for $d = 3$, $\Lambda = 0.84$ with $\chi = 0.91 \pm 0.02$ from linear fit, and $\chi = 1.39$ from theory. In the cases where the hypothesis of maximum entropy production, χ establishes the upper boundary for Γ . In the figures, the shaded regions indicate these forbidden regions. In both cases, $\Gamma_{MF} = \eta/d$ is shown. (b) The analytical solutions to $\Lambda(d)$ (top) and $\Gamma_0(d) = \Lambda(d)/d$ (bottom), as given by Eq. (3.6), are in great agreement with the data (Table 3 in Appendix A) and theory. (c) Final theoretical and numerical solutions to $D(d, \eta)$ for $d = 2$ and $d = 3$. (d) The theoretical solution for $D(d)$, shown as $\Delta D = D - (d - 1)$. For all the numerical values see Tables 3 and 4 in Appendix A.

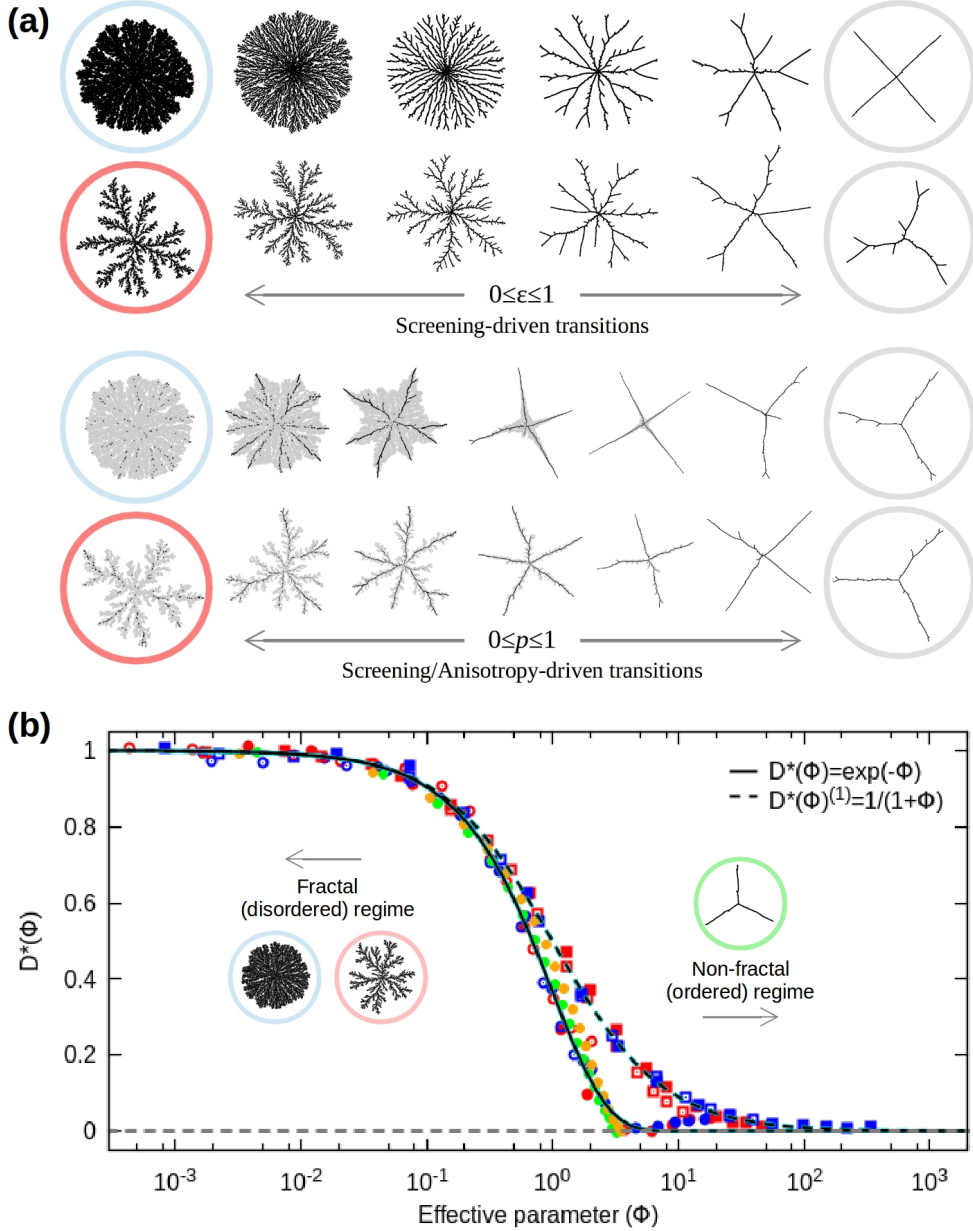


Figure 3.4: (a) Snapshots of typical clusters present in fractal to non-fractal morphological transitions obtained from the λ -model with the branching parameter ε as the control parameter, and the p -model with the mixing parameter p as the control parameter. (b) By plotting $D^*(\Phi)$ and $D^*(\Phi)^{(1)}$, the data for the morphological transitions DLA-MF, BA-MF, and DBM collapse to universal curves described by equations (3.1) and (3.2). Under this prescription, these universal fractal to non-fractal morphological transitions are independent of the initial fractal dimension, D_0 , the symmetry-breaking process that drives the transition, even crossover effects, and, quite remarkably, the Euclidean dimension, d , of its embedding space.

Chapter 4

Outcome

In summary, we present a novel framework for the scaling of morphological transitions in stochastic growth processes. By means of a general *ansatz* for an effective control parameter, Φ , we were able to construct a model for the fractal dimension D that describes the fractality of very different systems. In particular, this model is able to describe the scaling of the newly introduced BA/DLA-MF transitions, as well as it provides an excellent description for the fractal dimensions of the well-known DBM. In this case, an analytical solution was constructed that is in excellent agreement with numerical results reported over the years.

In addition, it was strictly shown that D can be used as a rotational-symmetry “order” parameter under the reduced co-dimension transformation D^* . On the other hand, we have shown that the previously suggested “critical” point for the DBM cannot be properly defined as such, but instead, as a transitional point in the fractality of a continuous morphological transition. These findings indicate that a quantification based on this rotational-symmetry would provide an important characterization of these morphological transitions.

Finally, we have shown that under the reduced co-dimension, the BA/DLA-MF and DBM transitions exhibit a well-defined universal scaling, $D^*(\Phi)$, that is remarkably independent of their initial configuration, the specific spatial symmetry-breaking mechanism that drives the transition, and the dimensionality of their embedding Euclidean space. The study and characterization of other morphological transitions available in the literature as well as new ones, such as the proposed controlled screened model, using the dimensionality function $D(\Phi)$ would be necessary to validate its generality.

In general, we consider that the results and models presented in this work represent a significant unifying step towards a complete scaling theory of fractal growth and far-from-equilibrium pattern formation. Additionally, the possibility of applying this model to discuss current issues in fractal growth-phenomena and other related research areas, ranging from biology [1, 3], intelligent materials engineering [34, 35] to medicine [36, 37, 38], seems to be more feasible and direct.

Appendix A. Fractal dimensions of DLA and DBM

Table 1: Numerical results for DLA in two dimensions. Results from standard numerical scaling analysis (first section) and multifractal analysis (second section). These include: density-density correlation (DDC), radius of gyration (RGy), mass-length (ML), radial density (RD), angular-gap distribution (AGD) and box-counting (BC) methods. Only off-lattice results are considered when available, otherwise lattice results are indicated (L). Specifications such as the number of clusters (C), and number of particles per cluster (N) used are shown. Any data not explicitly reported is indicated as NA (not available). Error in measurements shown when available.

(Year)	Author(s)	D	Method	Specifications
(1981)	Witten & Sander [43, 44]	1.657 ± 0.004	DDC	C=6, N≈ 3000 (L)
		1.673 ± 0.001	DDC	C=3, N≈ 3000 (L)
		1.70 ± 0.02	RGy	C=6, N≈ 3000 (L)
(1983)	Meakin [64, 65]	1.68 ± 0.03	DDC	C=4, N≈ 8500
		1.71 ± 0.07	RGy	
(1989)	Tolman & Meakin [66]	1.715 ± 0.004	RGy	C=377, N~ 10 ⁴ -10 ⁶
(1989)	Hinrichsen, <i>et al.</i> [45]	1.69 ± 0.01	ML	C=310, N~ 10 ³ -10 ⁵
		1.710 ± 0.005	RGy	
		1.712 ± 0.003	RD	C=10 ² , N~ 10 ⁵ -10 ⁶
(1991)	Ossadnik [46]	1.68	DDC	C=5, N= 25000
		1.71	RGy	
		1.67, 1.75	AGD	C=60, N=10 ⁸
(2001)	Huang [15]	1.723 ± 0.007	RGy	C=10 ³ , N=7 × 10 ⁶
(2002)	Mandelbrot, <i>et al.</i> [47]	1.71	RD	C=10 ³ , N=5 × 10 ⁷
(2012)	Menshutin [48]	1.711 ± 0.009	ML	C=4, N~ 10 ⁶ -10 ⁹
(2016)	Nicolás, <i>et al</i> [27]	1.710 ± 0.005	DDC	C=128, N=10 ⁵
		1.708 ± 0.013	RGy	
		1.683 ± 0.008	ML	
		1.608 ± 0.017	BC (q = 0)	C=10, N≈ 10 ⁴ (L)
(1984)	Meakin & Wasserman [49]	1.646 ± 0.009	BC (q = 2)	
		1.67 ± 0.03	BC (q = 0)	C=310, N~ 10 ³ -10 ⁵
(1989)	Hinrichsen, <i>et al.</i> [45]	1.69 ± 0.03	BC (Any q)	C=27, N=5 × 10 ⁴
(1989)	Li, <i>et al.</i> [50]	1.60 ± 0.02	Wavelet (Any q)	C=NA, N~ 10 ⁴ (L)
(1990)	Argoul, <i>et al.</i> [51]	1.71	Sandbox (q = 2)	C=5, N=10 ⁶
(1990)	Vicsek, <i>et al.</i> [52]	1.65 ± 0.01	BC (q = 0)/ML	C=20, N=10 ⁶
(1995)	Mandelbrot, <i>et al.</i> [53]	1.697	Sandbox (Any q)	C=10 ² , N=10 ⁶
(2012)	Hanan & Heffernan [54]	1.7018	BC (q = 2)	C=4, N~ 10 ⁶ -10 ⁹
		1.70	BC (Any q)	

Table 2: **Theoretical results for DLA in two dimensions.** Results from diverse theoretical approaches are presented. Only off-lattice results are considered, otherwise is indicated.

(Year)	Author(s)	$D \simeq 1.67$	$D \simeq 1.71$	Method
(1983)	Muthukumar [75]	$5/3 \simeq 1.67$		Mean-field (MF) approach
(1984)	Tokuyama & Kawasaki [76]	$5/3 \simeq 1.67$		MF approach
(1984)	Hentschel [72]		$7/4 = 1.75$	Flory-type approach
(1985)	Turkevich & Scher [69]	$5/3 \simeq 1.67^a$	$7/4 = 1.75^b$	Occupancy-probability scaling
(1986)	Ball [55]		$1 + \sqrt{2}/2 \simeq 1.707$	Cone angle theory
(1986)	Halsey, <i>et al.</i> [56]		1.705	Harmonic measure (HM) analysis
(1986)	Honda, <i>et al.</i> [22, 23]	$5/3 \simeq 1.67$		MF approach
(1987)	Nagatani [57]		1.711	Renormalisation-group (RG) approach
(1988)	Amitrano, <i>et al.</i> [58]	1.69 ± 0.01	1.737	RG approach
(1992)	Wang & Huang [74]			RG approach
(1994)	Halsey [71]			Branch competition model
(1995)	Pietronero & Erzan [9, 70]	1.661	1.71	Fixed scale transformation
(1997)	Hastings [59]		$1+1/2+1/5 = 1.70$	RG approach
(1997)	Hayakawa & Sato [60]		1.701	History probability
(2000)	Davidovitch, <i>et al.</i> [61]		1.713 ± 0.003	Conformal mapping (Cluster)
(2001)	Davidovitch, <i>et al.</i> [62]		1.71	Conformal mapping (HM)
(2002)	Ball & Somfai [63]	$1+2/3 \simeq 1.67$		Gaussian-closure approx. for HM

^aSquare lattice

^bTriangular lattice

Table 3: DLA dimensions. First section: numerical results for $D(d, \eta = 1)$ with the corresponding average, $\langle D(d) \rangle$. Clusters grown off-lattice marked with ‘*’, while the rest are for a square lattice. Second section: theoretical results are compared to $D(d)_{MF}$ and $D(d)$ obtained by the theory (T). Error in measurements shown when available.

Source	$d = 2$	$d = 3$	$d = 4$	$d = 5$	$d = 6$	$d = 7$	$d = 8$
Rodriguez & Sosa [67]	$1.711 \pm 0.008^*$	$2.51 \pm 0.01^*$					
Meakin [64, 65]	$1.71 \pm 0.07^*$	$2.50 \pm 0.08^*$					
Tolman & Meakin [66]	1.71 ± 0.05	2.51 ± 0.06	3.32 ± 0.10				
$\langle D(d) \rangle$	1.70 ± 0.06	2.53 ± 0.06	3.31 ± 0.10	4.20 ± 0.16	≈ 5.35		
Turkevich & Scher [69]	$1.715 \pm 0.004^*$	2.495 ± 0.005	≈ 3.40	≈ 4.33	≈ 5.40	≈ 6.45	≈ 7.50
Erzan, <i>et al.</i> [70]	1.67	2.46					
Halsey [71]	1.71	2.54					
Hentschel [72]	1.66	2.50	3.40	4.33			
$D(d)_{RG}$ [73, 74]	1.75	2.52	3.38	4.29	5.0		
$D(d)$ (T)	1.74	2.52	3.34	4.22	5.13	6.08	7.05
$D(d)_{MF}$	1.71	2.50	3.32	4.12	5.11	6.07	7.04
	1.67	2.50	3.40	4.33	5.29	6.25	7.22

Table 4: DBM dimensions. Full set of data for the average dimension, $\langle D(d, \eta) \rangle$, for $d = 2$ and $d = 3$, is compared to $D(d, \eta)_{MF}$ and $D(d, \eta)$ as obtained by the theory (T) and by a direct fit (F) to data. Data sources marked with '*' are not considered in the average due to known limitations in their measurements. Errors are shown when available.

Source	$\eta = 0.5$	$\eta = 1$	$\eta = 2$	$\eta = 3$	$\eta = 4$	$\eta = 5$
Niemeyer, <i>et al.</i> [8]*	1.89 ± 0.01	1.75 ± 0.02	1.6			
Hayakawa, <i>et al.</i> [24]*	1.79 ± 0.01		1.47 ± 0.03			
Pietronero, <i>et al.</i> [9]	1.92	1.70	1.43			
Somfai, <i>et al.</i> [25]		1.71	1.42	1.23		
Tolman & Meakin [40]						
Sánchez, <i>et al.</i> [20]*	1.86	1.61	1.35	1.22	1.08	1.04
Amitrano [26]		1.69	1.43	1.26	1.16	1.07
Hastings [21]			1.433	1.263	1.128	1.068
			1.426	1.264	1.090	1.030
			1.435	1.262	1.078	1.025
			1.452	1.243	1.071	1.009
$\langle D(\eta, d=2) \rangle$	1.89 ± 0.05	1.70 ± 0.01	1.43 ± 0.02	1.26 ± 0.02	1.11 ± 0.04	1.04 ± 0.03
$D(\eta, d=2)$ (F)	1.87	1.71	1.41	1.22	1.10	1.05
$D(\eta, d=2)$ (T)	1.88	1.71	1.37	1.16	1.06	1.02
$D_{MF}(\eta, d=2)$	1.80	1.67	1.50	1.40	1.33	1.29
Satpathy [41]						
	2.48 ± 0.06	2.11 ± 0.06	1.96 ± 0.08	1.75 ± 0.06		
	2.54 ± 0.06	2.09 ± 0.06	1.84 ± 0.07	1.79 ± 0.08		
Tolman & Meakin [40]	2.50 ± 0.10	2.134 ± 0.001	1.895 ± 0.004			
Vespignani & Pietronero [42]		2.13 ± 0.10	1.89 ± 0.10			
	2.49	2.17	1.91			
	2.54	2.21	1.92			
$\langle D(\eta, d=3) \rangle$						
$D(\eta, d=3)$ (F)	2.51 ± 0.03	2.14 ± 0.04	1.90 ± 0.04	1.77 ± 0.03		
$D(\eta, d=3)$ (T)	2.50	2.18	1.93	1.75		
$D_{MF}(\eta, d=3)$	2.50	1.94	1.53	1.27		
	2.50	2.20	2.00	1.86		

Appendix B. Models and methods

Aggregation dynamics

In all simulations, each particle has a diameter equal to one. This is the basic unit of distance of the system. For aggregates based on BA or MF (Figs. 1a and 1c), we follow a standard procedure in which particles are launched at random from a circumference of radius $r_L = 2r_{max} + \delta$, with equal probability in position and direction of motion. Here, r_{max} is the distance of the farthest particle in the cluster with respect to the seed particle placed at the origin. In our simulations we used $\delta = 1000$ particle diameters to avoid undesired screening effects. For the MF model, particles always aggregate to the closest particle in the cluster with respect to their incoming path. This is determined by the projected position of the aggregated particles along the direction of motion of the incoming particle (see Fig. 1c). In the case of aggregates based on DLA (Fig. 1b), particles were launched from a circumference of radius $r_L = r_{max} + \lambda + \delta$, for the λ -model, and $r_L = r_{max} + \delta$, for the p -model, with $\delta = 100$ in both cases. The mean free path of the particles is set to one particle diameter. We also used a standard scheme that modifies the mean free path of the particles as they wander at a distance larger than r_L or in-between branches, as well as the common practice of setting a killing radius at $r_K = 2r_L$ in order to speed up the aggregation process.

In order to mix different aggregation dynamics, a Monte Carlo scheme of aggregation is implemented using the BA, DLA and MF models. The combination between pairs of models results in the DLA-MF and BA-MF transitions, controlled by the mixing parameter $p \in [0, 1]$, associated with the probability or fraction of particles aggregated under MF dynamics, $p = N_{MF}/N$, where N is total number of particles in the cluster. Therefore, as p varies from $p = 0$ (pure stochastic dynamics given by the BA or DLA models) to $p = 1$ (purely energetic dynamics given by the MF model), it generates the two transitions introduced in the work. The evaluation of the aggregation scheme to be used is only updated once a particle has been successfully

aggregated to the cluster under such dynamics.

Fractal and scaling analysis

In all of the measurements, we used 128 clusters containing 1.5×10^5 particles. Formally, the fractal dimension is measured from the two-point density correlation function, $C(r) = \langle\langle \rho(\mathbf{r}_0)\rho(\mathbf{r}_0 + \mathbf{r}) \rangle\rangle_{|\mathbf{r}|=r}$, where the double bracket indicates an average over all possible origins \mathbf{r}_0 and all possible orientations. For this work, we made use of 1000 possible origins. Here, it is assumed that $C(r) \approx r^{-\alpha}$, where the fractal dimension is given by $D_\alpha = d - \alpha$, where d is the dimension of the embedding space. We also used the radius of gyration given by $R_g^2 = \sum_{i=1}^N (\mathbf{r}_i - \mathbf{r}_{CM})^2$, where N is the number of particles, \mathbf{r}_i is the position of the i th-particle in the cluster, and, \mathbf{r}_{CM} is the position of the center of mass. In this scheme, it is assumed that $R_g(N) \approx N^\beta$, where the fractal dimension is given by $D_\beta = 1/\beta$. Therefore, the fractal dimensions, D_α and D_β , are respectively obtained from linear-fits to the corresponding functions, $C(r)$ and $R_g(N)$, in log-log plots for different scales. In practice, it is assumed that α and β are constant as long as the size or number of particles in the cluster is large enough. However, because the clusters do not develop a constant scaling, alternative methods were used in order to capture their main local fractal features.

For the λ -model, the derivative of R_g in the logarithmic scale was computed by means of standard two and three point numerical differentiation methods: $f'(x) = [f(x+h) - f(x)]/h$, at the end of the differentiation intervals, and $f'(x) = [f(x+h) - f(x-h)]/2h$, in between. Here $f(x) = \log R_g(N)$ and $R_g(N)$ are computed as a discrete quantity therefore, h is set as the distance between the points, $x = x_j$ and $x + h = x_{j+1}$. In all cases, R_g is computed as an average over a large ensemble of aggregates. Specifically, the results for the multiscaling aggregates were obtained over 64 and 15 aggregates containing 1.5×10^5 and 3×10^5 particles for those based on DLA and BA, respectively. In this case, R_g was calculated every 10 particles. The results for tunable aggregates based on DLA and BA were obtained over 128 and 48 aggregates, respectively, containing 10^5 particles, and R_g was computed every 10 particles.

In the case of the p -model, linear-fits at different scales were performed and averaged over a sample of 10 measurements, distributed over a given interval in order to improve the precision. For both transitions, DLA-MF and BA-MF, $D_\alpha(p)$ is measured at short length-scales (this is α_I) over the interval $r_i \in [1, 2]$ with fitting-length equal to 10, and $r_f \in [11, 12]$ (in particle diameters units). At long length-scales (α_{II}), over $r_i \in [10, 11]$ with fitting-length equal to 40, and $r_f \in [50, 51]$. On the other hand, for $D_\beta(p)$, the measurements at medium scales (β_I) were performed over the interval $r_i \in [10^2, 10^3]$ with fitting-length equal to 10^4 and $r_f \in [1.01 \times 10^4, 1.1 \times 10^4]$ (in

particle number), while, at large scales (β_{II}), over the interval $r_i \in [10^3, 10^4]$ with fitting-length equal to 0.9×10^5 and $r_f \in [9.1 \times 10^4, 10^5]$.

Appendix C. Additional preliminary results

Mean field effect on angular correlation

This work in progress is in collaboration with Juan Manuel Solano-Altamirano, at Facultad de Ciencias Químicas, BUAP. A manuscript entitled “Mean field effect on angular correlation and fractal growth in small clusters” by J. R. Nicolás-Carlock, J. M. Solano-Altamirano, and J. L. Carrillo-Estrada, is in preparation.

To measure the angular correlation, $c_R(\theta)$, we used $RdRd\theta \approx N\pi/4$, and the average is normalized to the number of boxes used to count particles within the ring $R - \delta R/2 < r < R + \delta R/2$. The size of the counting box is evaluated as follows:

$$\frac{N\pi}{4} = \frac{fR^2 \cdot 2\pi}{K} \Rightarrow K = \frac{8fR^2}{N}. \quad (1)$$

Here, N is some number of particles (determined heuristically), K determines $d\theta$, $d\theta = 2\pi/K$, and f sets dR , $dR = fR$. For the calculations presented here, we used $N = 3$ and $f = 0.1$ for computing $c_R(\theta)$, $R = 7, 9, 11, 13, 15$; $N = 10$ and $f = 0.1$ for computing $c_R(\theta)$, $R = 20, 40, 60, 80$ and $N = 25$; and $f = 0.05$ for computing $c_R(\theta)$, $R = 100, 125, 150, 175, 200$.

In small clusters, *i.e.* clusters whose radii are $<\sim 40d$ (here d is the a particle diameter), the shape of the $c_R(\theta)$ vs θ curves are more similar (as p increases) than the shapes of the same curves at larger radius ($>\sim 40d$), see Fig. 1 for BA/MF and Fig. 3 for DLA/MF.

This conclusion can also be deducted from the exponents of the scaling law (see Fig. 2 for BA/MF and Fig. 4 for DLA/MF).

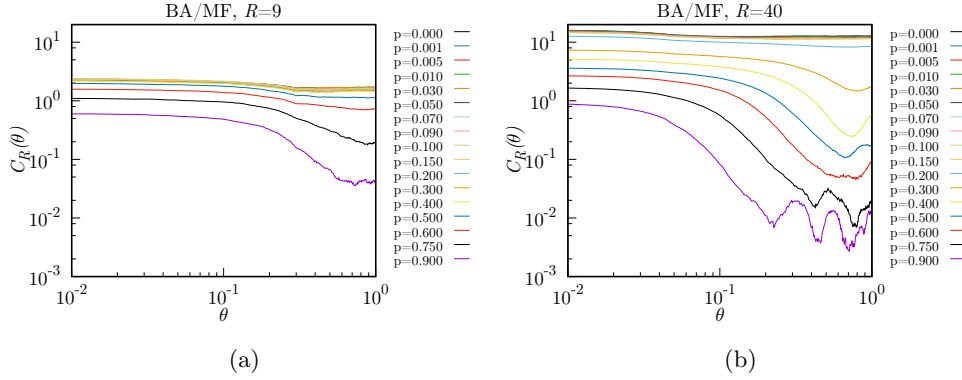


Figure 1: Log-log plot of $c_R(\theta)$ vs θ for different values of p , where p is the degree of mixing BA/MF. As the MF character of the cluster increases, the angular correlation decays progressively earlier, *i.e.* at lower p values.

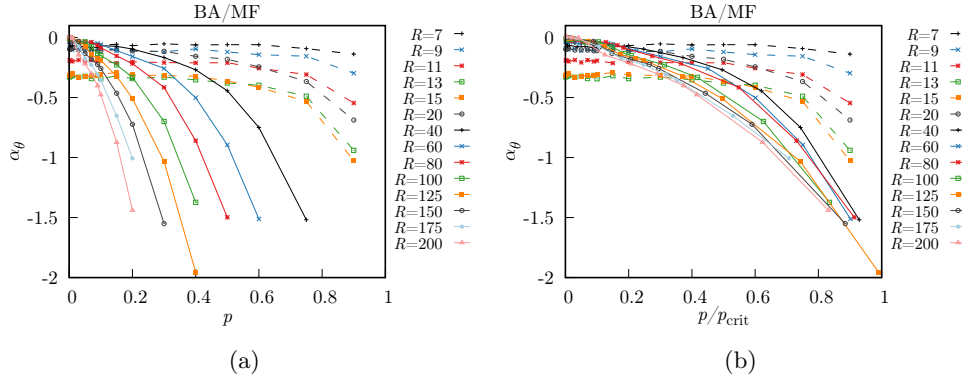


Figure 2: Exponent p -evolution measured at different values of R . α_θ vs p , and α_θ vs p_{red} . Here p is the degree of mixing BA/MF, and $p_{\text{red}} \equiv p/p_{\text{crit}}$, where p_{crit} is the interpolated value of p such that $\alpha_\theta(p_{\text{crit}}) = -2$. For $R > 20$ the clusters reflect the MF contribution to their growth. The behaviour seems to be quasi-universal relative to p_{red} .

Controlled screening model of particle aggregation

This is a work in progress. A manuscript entitled “Fractal growth by controlled screening in particle-cluster aggregation” by J. R. Nicolás-Carlock, V. Dossetti, and J. L. Carrillo-Estrada, is in preparation.

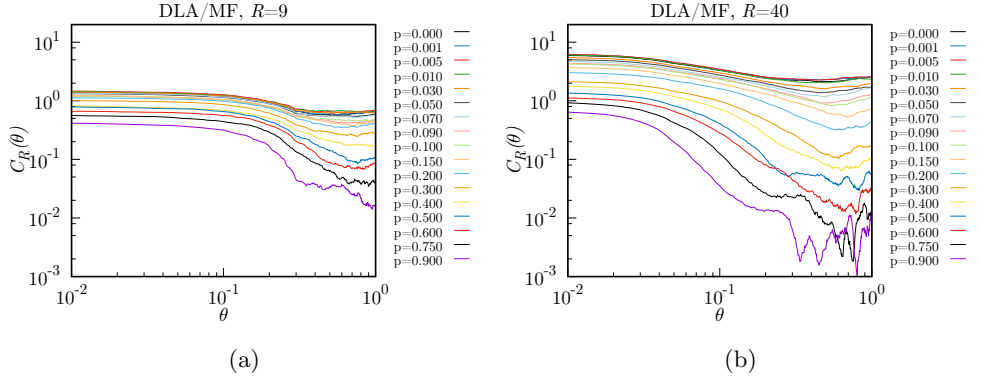


Figure 3: Log-log plot of $c_R(\theta)$ vs θ for different values of p , where p is the degree of mixing DLA/MF. As the MF character of the cluster increases, the angular correlation decays progressively earlier, *i.e.* at lower p values.

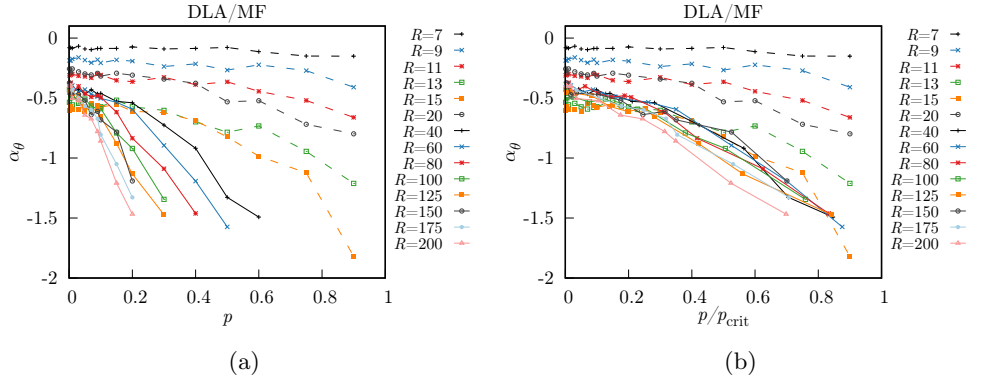


Figure 4: Exponent p -evolution measured at different values of R . (a) α_θ vs p , and (b) α_θ vs p_{red} . Here p is the degree of mixing DLA/MF, and $p_{\text{red}} \equiv p/p_{\text{crit}}$, where p_{crit} is the interpolated value of p such that $\alpha_\theta(p_{\text{crit}}) = -2$. For $R > 20$ the clusters reflect the MF contribution to their growth. The behaviour seems to be quasi-universal relative to p_{red} .

This particle-cluster aggregation model is based on the concept of penetration length, l , the effective distance that characterizes the region to which particles are able to aggregate within a growing cluster. For example, aggregated particles in BA form a compact cluster that does not allow a deep penetration into its inner structure, therefore its penetration length is almost zero. In a DLA cluster, aggregated particles form big branches, allowing a deeper penetration into the structure. In the

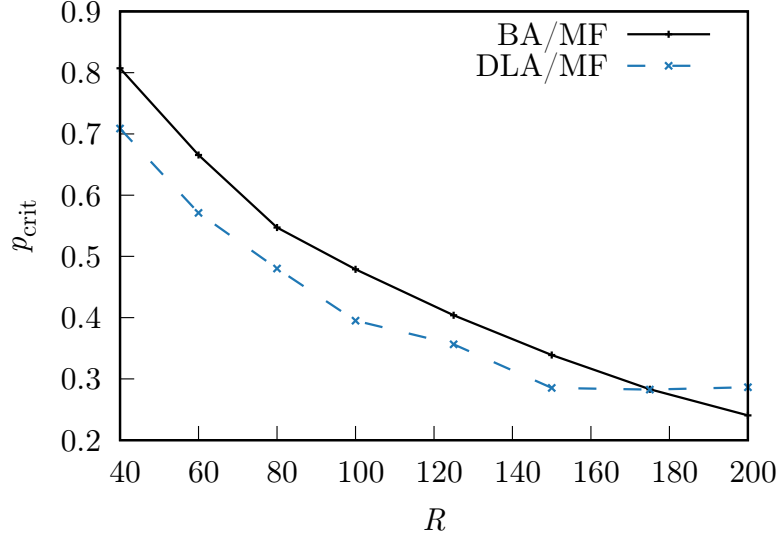


Figure 5: The critical p as a function of R . Here p is the degree of mixing BA/MF (or DLA/MF), R is the radius whereat the angular correlation is measured, and p critical (denoted as p_{crit}) is the value of p whose scaling-law exponent is $\alpha_\theta(p_{\text{crit}}) = -2$.

MF scenario, the penetration length goes again to zero because the particles aggregate to the outermost parts of the cluster, this is, the tips. Within mean-field theories [23], the penetration length is given as,

$$l \propto r^\delta, \quad \delta = \frac{d - D}{d_w - 1}, \quad (2)$$

where r is the distance from the center of the cluster. However, this expression is expected to provide an approximation to the real functional relation among variables.

This length also characterizes the active region in the growing front that is in charge on defining the fractality of the cluster as stated in the Turkevich-Scher relation, $D = 1 + \alpha$, therefore the importance of its systematic study. To this end, we introduce a new model of particle-cluster aggregation in which particles following BA or DLA dynamics are allowed to aggregate only within a portion of the growing front as defined ξ , and controlled by the parameter $\zeta \in [0, 1]$, as giving by $\xi \propto r^\zeta$, where r is the size of the cluster, see Fig. 6.

The main objectives of this study are to explore the origins of fractality in this new model of particle aggregation, to test the limits of δ and provide an analytical solution using our generalized dimensionality function $D(\Phi)$, and test again the generality of the Turkevich-Scher conjecture.

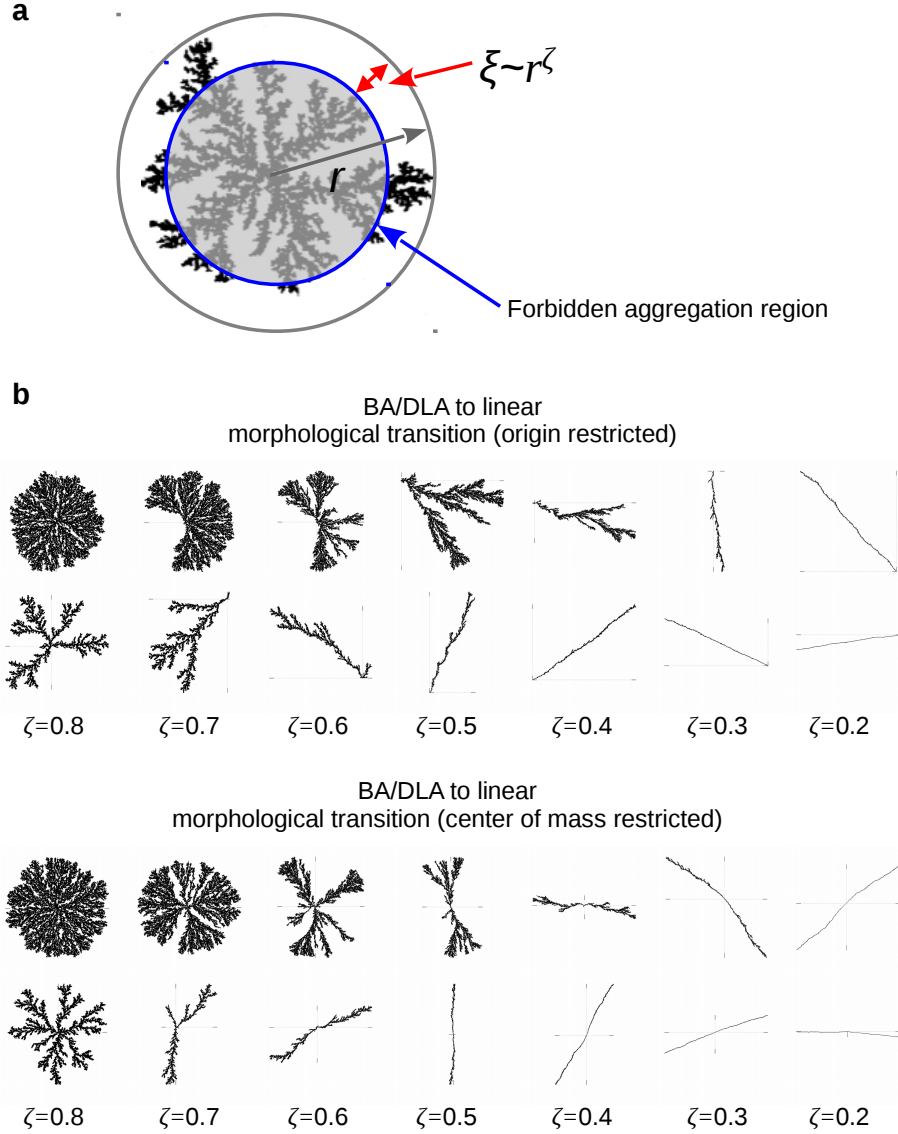


Figure 6: (a) The screened model of aggregation. Particles can follow either DLA or BA dynamics before aggregation takes place outside the forbidden region. (b) There are two variants of this model for each aggregation dynamics. First, aggregation restricted to the origin or seed particle, and aggregation restricted to the center of mass. Different morphologies and symmetries appear as function of these rules. In all cases, $D = D_0$, for the initial states with unrestricted BA or DLA dynamics for $\zeta = 1$, and $D \rightarrow 1$ as $\zeta \rightarrow 0$. For each value of ζ shown there are 120 clusters containing up to 100 thousand particles.

Bibliography

- [1] Ben-Jacob, E. From snowflake formation to growth of bacterial colonies. Part I. Diffusive patterning in azoic systems. *Contemp. Phys.* **34**, 247–273 (1993).
- [2] Ben-Jacob, E. From snowflake formation to growth of bacterial colonies. Part II. Cooperative formation of complex colonial patterns. *Contemp. Phys.* **38**, 205–241 (1997).
- [3] Vicsek, T. *Fluctuations and Scaling in Biology* (OUP Oxford, 2001).
- [4] Ronellenfitsch, H. & Katifori, E. Global Optimization, Local Adaptation, and the Role of Growth in Distribution Networks. *Phys. Rev. Lett.* **117**, 138301 (2016).
- [5] Ben-Jacob, E. & Garik, P. The Formation of Patterns in non equilibrium growth. *Nature* **343**, 523–530 (1990).
- [6] Vicsek, T. *Fractal Growth Phenomena* (World Scientific, Singapore, 1992).
- [7] Meakin, P. *Fractals, Scaling and Growth Far from Equilibrium* (Cambridge University Press, Cambridge, 1998).
- [8] Niemeyer, L., Pietronero, L. & Wiesmann, H. J. Fractal Dimension of Dielectric Breakdown. *Phys. Rev. Lett.* **52**, 1033 (1984).
- [9] Pietronero, L., Erzan, A. & Evertsz, C. Theory of Fractal Growth. *Phys. Rev. Lett.* **61**, 861 (1988).
- [10] Sander, L. M. Fractal growth processes, *Nature* **322**, 789–793 (1986).
- [11] Sander, L. M. Diffusion-limited aggregation: A kinetic critical phenomenon? *Contemp. Phys.* **41**, 203–218 (2000).
- [12] Sander, L. M. Fractal growth processes, in *Mathematics of Complexity and Dynamical Systems* (ed. Meyers, R. A.) pp. 429–445 (Springer, New York, 2011).

- [13] Meakin, P. Effects of particle drift on diffusion-limited aggregation. *Phys. Rev. B* **28**, 5221 (1983).
- [14] Huang, Y.-B. & Somasundaran, P. Effects of random-walk size on the structure of diffusion-limited aggregates. *Phys. Rev. A* **36**, 4518–4521 (1987).
- [15] Huang, S.-Y., Zou, X.-W., Tan, Z.-J. & Jin, Z.-Z. Particle-cluster aggregation by randomness and directive correlation of particle motion. *Phys. Lett. A* **292**, 141–145 (2001).
- [16] Ferreira Jr., S. C., Alves, S. G., Faissal Brito, A. & Moreira, J. G. Morphological transition between diffusion-limited and ballistic aggregation growth patterns. *Phys. Rev. E* **71**, 051402 (2005).
- [17] Alves, S. G. & Ferreira Jr., S. C. Aggregation in a mixture of Brownian and ballistic wandering particles. *Phys. Rev. E* **73**, 051401 (2006).
- [18] Meakin, P. Cluster-particle aggregation with fractal (Levy flight) particle trajectories. *Phys. Rev. B* **29**, 3722 (1984).
- [19] Mathiesen, J. & Jensen, M. H. Tip Splitting and Phase Transitions in the Dielectric Breakdown Model: Mapping to the Diffusion-Limited Aggregation Model. *Phys. Rev. Lett.* **88**, 235505 (2002).
- [20] Sánchez, A., Guinea, F., Sander, L. M., Hakim, V. & Louis, E. Growth and forms of Laplacian aggregates. *Phys. Rev. E* **48**, 1296 (1993).
- [21] Hastings, M. B. Fractal to Nonfractal Phase Transition in the Dielectric Breakdown Model. *Phys. Rev. Lett.* **87**, 175502 (2001).
- [22] Honda, K., Toyoki, H. & Matsushita, M. A Theory of Fractal Dimensionality for Generalized Diffusion-Limited Aggregation. *J. Phys. Soc. Jpn.* **55**, 707–710 (1986).
- [23] Matsushita, M., Honda, K., Toyoki, H., Hayakawa, Y. & Kondo, H. Generalization and the Fractal Dimensionality of Diffusion-Limited Aggregation. *J. Phys. Soc. Jpn.* **55**, 2618–2626 (1986).
- [24] Hayakawa, Y., Kondo, H. & Matsushita, M. Monte Carlo Simulations of the Generalized Diffusion-Limited Aggregation. *J. Phys. Soc. Jpn.* **55**, 2479–2482 (1986).
- [25] Somfai, E., Goold, N. R. & Ball, R. C. Growth by random walker sampling and scaling of the dielectric breakdown model. *Phys. Rev. E* **70**, 051403 (2004).

- [26] Amitrano, C. Fractal dimensionality for the η model. *Phys. Rev. A* **39**, 6618 (1989).
- [27] Nicolás-Carlock, J. R., Carrillo-Estrada, J. L. & Dossetti, V. Fractality à la carte: a general particle aggregation model. *Sci. Rep.* **6**, 19505 (2016).
- [28] J. R. Nicolás-Carlock, V. Dossetti, and J. L. Carrillo-Estrada, “Universal fractality of morphological transitions in stochastic growth processes” *Scientific Reports* (2017) [ACCEPTED].
- [29] J. R. Nicolás-Carlock, V. Dossetti, and J. L. Carrillo-Estrada, “Fractal to non-fractal morphological transitions in stochastic growth processes”, in *Fractal Analysis - Applications in Health Sciences and Social Sciences* (ed. F. Brambila) Intech (2017) [ACCEPTED].
- [30] Dimino, G. M. & Kaufman, J. H. Evidence of Critical Behavior in a Random Fractal Automaton. *Phys. Rev. Lett* **62**, 2277 (1989).
- [31] Kaufman, J. H., Dimino, G. M. & Meakin, P. Universality of Critical Screening in the Formation of Fractal Patterns. *Phys. A* **157**, 656-668 (1989).
- [32] Jullien, R. A. A new model of cluster aggregation. *J. Phys. A: Math. Gen.* **19**, 2129 (1986).
- [33] Mathiesen, J., Procaccia, I., Swinney, H. L. & Thrasher, M. The universality class of diffusion-limited aggregation and viscous fingering. *Europhys. Lett.* **72**, 257–263 (2006).
- [34] Lehn, J-M. Toward Self-Organization and Complex Matter, *Science* **295**, 2400 (2002).
- [35] Whitesides, G. M. & Grzybowski, B. Self-Assembly at All Scales, *Science* **295**, 2418 (2002).
- [36] Sturmberg, J. P. & West, B. J., Fractals in Physiology and Medicine. in *Handbook of Systems and Complexity in Health* (ed. Sturmberg, J. P. & Martin, C. M.) pp. 171–192 (Springer New York, 2013).
- [37] Lennon, F. E. *et al.* Lung cancer—a fractal viewpoint. *Nat. Rev. Clin. Oncol.* **12**, 664–675 (2015).
- [38] Lennon, F. E. *et al.* Unique fractal evaluation and therapeutic implications of mitochondrial morphology in malignant mesothelioma. *Sci. Rep.* **6**, 24578 (2016).

- [39] Di Ieva, A. The Fractal Geometry of the Brain. *Springer series in computational neuroscience*, edited by A. Di Ieva (Springer, 2016).
- [40] Tolman, S. & Meakin, P. Two, three and four-dimensional diffusion-limited aggregation models. *Phys. A* **158**, 801 (1989).
- [41] Satpathy, S. Dielectric breakdown in three dimensions: results of numerical simulations. *Phys. Rev. B* **33**, 5093 (1986).
- [42] Vespignani, A. & Pietronero, L. Fixed scale transformation applied to diffusion limited aggregation and dielectric breakdown model in three dimensions. *Phys. A* **173**, 1 (1993).
- [43] Witten Jr., T. A. & Sander, L. M. Diffusion-Limited Aggregation, a Kinetic Critical Phenomenon. *Phys. Rev. Lett.* **47**, 1400 (1981).
- [44] Witten Jr., T. A. & Sander, L. M. Diffusion-Limited Aggregation. *Phys. Rev. B* **27**, 5686 (1983).
- [45] Hinrichsen, E. L. *et al.* Self-similarity and structure of DLA and viscous fingering clusters. *J. Phys. A: Math. Gen.* **22**, L271 (1989).
- [46] Ossadnik, P. Multiscaling analysis of large-scale off-lattice DLA. *Phys. A* **176** 454- 462 (1991).
- [47] Mandelbrot, B., Kol, B. & Aharony, A. Angular Gaps in Radial Diffusion-Limited Aggregation: Two Fractal Dimensions and Nontransient Deviations from Linear Self-Similarity. *Phys. Rev. Lett.* **88** 055501 (2002).
- [48] Menshutin, A. Scaling in the Diffusion Limited Aggregation Model. *Phys. Rev. Lett.* **108** 015501 (2012).
- [49] Meakin, P. & Wasserman, Z. Fractal Structure of Three-Dimensional Witten-Sander Clusters. *Chem. Phys.* **91**, 391 (1984).
- [50] Li,G, *et al.* Comment on Self-Similarity of Diffusion-Limited Aggregates and Electrodeposition Clusters. *Phys. Rev. Lett.* **63** 1322 (1989).
- [51] Argoul, F. *et al.* Wavelet analysis of the self-similarity of diffusion-limited aggregates and electrodeposition clusters. *Phys. Rev. A* **41** 5537 (1990).
- [52] Vicsek, T., Family, F. & Meakin, P., Multifractal Geometry of Diffusion-Limited Aggregates. *Europhys. Lett.* **12** 217 (1990).

- [53] Mandelbrot, B. B., Vespignani, A. & Kaufman, H. Crosscut Analysis of Large Radial DLA: Departures from Self-Similarity and Lacunarity Effects. *Europhys. Lett.* **32** 199 (1995).
- [54] Hanan, W. G. & Heffernan, D. M. Multifractal analysis of the branch structure of diffusion-limited aggregates. *Phys. Rev. E* **85** 021407 (2012).
- [55] Ball, R. C. Diffusion-limited aggregation and its response to anisotropy. *Physica A* **140**, 62 (1986).
- [56] Halsey, T. C., Meakin, P. & Procaccia, I. Scaling Structure of the Surface Layer of Diffusion-Limited Aggregates. *Phys. Rev. Lett.* **56**, 854 (1986).
- [57] Nagatini, T. A renormalisation group approach to the scaling structure of diffusion-limited aggregation. *J. Phys. A* **20**, L381 (1987).
- [58] Amitrano, C., Coniglio, A. & diLiberto, F. Static and dynamic properties for growth models. *J. Phys. A* **21**, L201 (1988).
- [59] Hastings, M. B. Renormalization theory of stochastic growth. *Phys. Rev. E* **55**, 135 (1997).
- [60] Hayakawa, Y. & Sato, S. Statistical Theory of Diffusion-Limited Growth in Two Dimensions. *Phys. Rev. Lett.* **79**, 95 (1997).
- [61] Davidovitch, B., Levermann, A. & Procaccia, I. Convergent calculation of the asymptotic dimension of diffusion limited aggregates: scaling and renormalization of small clusters. *Phys. Rev. E* **62** R5919 (2000).
- [62] Davidovitch, B. *et al.* Thermodynamic Formalism of the Harmonic Measure of Diffusion Limited Aggregates: Phase Transition *Phys. Rev. Lett.* **87** 164101 (2001).
- [63] Ball, R. C. & Somfai, E. Theory of Diffusion Controlled Growth. *Phys. Rev. Lett.* **89**, 135503 (2002).
- [64] Meakin, P. Diffusion-controlled cluster formation in two, three, and four dimensions. *Phys. Rev. A* **27**, 604 (1983).
- [65] Meakin, P. Diffusion-controlled cluster formation in 2-6 dimensional space. *Phys. Rev. A* **27**, 1495 (1983).
- [66] Tolman, S. & Meakin, P. Off-lattice and hypercubic-lattice models for diffusion-limited aggregation in the dimensionalities 2-8. *Phys. Rev. A* **40**, 428 (1989).

- [67] Rodriguez-Romo, S. & Sosa-Herrera, A. Lacunarity and multifractal analysis of the large DLA mass distribution. *Phys. A* **392**, 3316 (2013).
- [68] R. C. Ball and T. A. Witten, Particle Aggregation versus Cluster Aggregation in High Dimensions. *J. Stat. Phys.* **36**, 873 (1984).
- [69] Turkevich, L. A. & Scher, H. Occupancy-Probability Scaling in Diffusion-Limited Aggregation. *Phys. Rev. Lett.* **55**, 1026 (1985).
- [70] Erzan, L., Pietronero, L. & Vespignani, A. The fixed-scale transformation approach to fractal growth. *Rev. Mod. Phys.* **67** 545 (1995).
- [71] Halsey, T. C., Diffusion-Limited Aggregation as Branched Growth. *Phys. Rev. Lett.* **72**, 1228 (1994).
- [72] Hentschel, H. G. E. Fractal dimension of Generalized Diffusion-Limited Aggregates. *Phys. Rev. Lett.* **52**, 212 (1984).
- [73] X. R. Wang, Y. Shapir, and M. Rubinstein, *Phys. Lett. A* **138**, 274 (1989).
- [74] Wang, X. Z. & Huang, Y. Calculation of the fractal dimension of diffusion-limited aggregation by the normalisation-group approach in an arbitrary Euclidean dimension d . *Phys. Rev. A* **46** 5038 (1992).
- [75] Muthukumar, M. Mean-Field Theory for Diffusion-Limited Cluster Formation. *Phys. Rev. Lett.* **50**, 839 (1983).
- [76] Tokuyama, M. & Kawasaki, K. Fractal dimensions for diffusion-limited aggregation. *Phys. Lett.* **100A**, 337 (1984).
- [77] Kaufman, J. H., Melroy, O. R., and Dimino, G. M. *Phys. Rev. A* **39**, 1420 (1989).
- [78] Kaufman, J. H. and Dimino, G. M. *Phys. Rev. A* **39**, 6045 (1989).
- [79] Gleiser, M. and Sowinski, D. Information-entropic signature of the critical point. *Phys. Lett. B* **747**, 125 (2015).
- [80] Mathiesen, J., Jensen, M. H. & Bakk, J. Ø. H. Dimensions, maximal growth sites, and optimization in the dielectric breakdown model. *Phys. Rev. E* **77**, 066203 (2008).

SCIENTIFIC REPORTS



OPEN

Fractality à la carte: a general particle aggregation model

J. R. Nicolás-Carlock¹, J. L. Carrillo-Estrada¹ & V. Dossetti^{1,2}

Received: 11 September 2015

Accepted: 14 December 2015

Published: 19 January 2016

In nature, fractal structures emerge in a wide variety of systems as a local optimization of entropic and energetic distributions. The fractality of these systems determines many of their physical, chemical and/or biological properties. Thus, to comprehend the mechanisms that originate and control the fractality is highly relevant in many areas of science and technology. In studying clusters grown by aggregation phenomena, simple models have contributed to unveil some of the basic elements that give origin to fractality, however, the specific contribution from each of these elements to fractality has remained hidden in the complex dynamics. Here, we propose a simple and versatile model of particle aggregation that is, on the one hand, able to reveal the specific entropic and energetic contributions to the clusters' fractality and morphology, and, on the other, capable to generate an ample assortment of rich natural-looking aggregates with any prescribed fractal dimension.

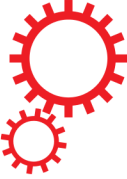
From the formation of mineral veins, complex biopolymers to clusters of galaxies, aggregation phenomena are out-of-equilibrium processes of fractal pattern formation ubiquitous in nature^{1–3}. Since the appearance of the diffusion-limited aggregation⁴ (DLA) and ballistic aggregation⁵ (BA) models, a plethora of studies have been developed trying to understand the ultimate aspects of the aggregation dynamics that give rise to *self-affine* or fractal clusters, the relationship of this fractality with their physical and chemical properties, and the most effective methods and techniques to control fractal growth^{6–8}.

Furthermore, these simple paradigmatic models, proposed as way to understand aggregation under *short-range* interactions, have contributed to reveal that the main sources of fractality in particle-cluster aggregation are related to the general entropic and energetic characteristics of the system. That is, when long-range interactions are negligible, the entropic information of the growing medium (such as its temperature and viscosity), encoded in the mean squared displacement of aggregating particles, is the main element of the dynamics that determines the fractality and morphology of the clusters. For example, random trajectories of the wandering particles in DLA generate branching clusters with fractal dimension $D < d$, where d is the dimension of the embedding space, whereas ballistic (straight line) trajectories in BA generate compact clusters with $D = d^{9–14}$. On the other hand, when attractive or repulsive interactions can no longer be disregarded, aggregation dynamics can become quite complex. Nonetheless, experimental results^{15–19} and computational models^{20–28} have shown that for short-range repulsive interactions, clusters tend to be compact with $D \approx d$. Conversely, long-range attractive interactions generate highly ramified clusters with a non-trivial fractal behavior characterized by $D \ll d$, as the range of the interactions becomes larger.

In the last case, fractality is enhanced by the branching growth process that emerges from screening effects generated by the aggregated particles^{29,30}, a fact that has led to consider that the main contribution to the fractality and morphology of the clusters is of an energetic character only, making the entropic one of no special significance but just as an intrinsic stochastic element of the dynamics^{20–24}. However, while screening and anisotropic effects might play an important role when interactions are present^{31–37}, in this Article we show that the entropic contribution cannot be trivially considered as this intrinsic stochastic element, but as an important aspect of the dynamics that contributes greatly to the fractality of the clusters, making it also a remarkable source of shape and texture in fractal pattern formation. To this end, through the incorporation of an effective interaction or aggregation range^{20,37}, λ , in the dynamics of the standard two-dimensional off-lattice particle-cluster DLA and BA models, we introduce a simple but non-trivial stochastic scheme that allows one to separate and characterize the subtle contributions of entropic and energetic character of the dynamics to the fractality and morphology of the clusters. This scheme also allows one to generate fractal clusters with rich morphological features, and most important, to harness absolute control over their fractal dimension.

¹Instituto de Física, Benemérita Universidad Autónoma de Puebla, Puebla, 72570, Mexico. ²CIDS-Instituto de Ciencias, Benemérita Universidad Autónoma de Puebla, Puebla, 72570, Mexico. Correspondence and requests for materials should be addressed to J.L.C.-E. (email: carrillo@ifuap.buap.mx)

SCIENTIFIC REPORTS



OPEN

Universal fractality of morphological transitions in stochastic growth processes

Received: 19 December 2016

Accepted: 28 April 2017

Published: xx xx xxxx

J. R. Nicolás-Carlock¹, J. L. Carrillo-Estrada¹ & V. Dossetti^{1,2}

Stochastic growth processes give rise to diverse and intricate structures everywhere in nature, often referred to as fractals. In general, these complex structures reflect the non-trivial competition among the interactions that generate them. In particular, the paradigmatic Laplacian-growth model exhibits a characteristic fractal to non-fractal morphological transition as the non-linear effects of its growth dynamics increase. So far, a complete scaling theory for this type of transitions, as well as a general analytical description for their fractal dimensions have been lacking. In this work, we show that despite the enormous variety of shapes, these morphological transitions have clear universal scaling characteristics. Using a statistical approach to fundamental particle-cluster aggregation, we introduce two non-trivial fractal to non-fractal transitions that capture all the main features of fractal growth. By analyzing the respective clusters, in addition to constructing a dynamical model for their fractal dimension, we show that they are well described by a general dimensionality function regardless of their space symmetry-breaking mechanism, including the Laplacian case itself. Moreover, under the appropriate variable transformation this description is universal, i.e., independent of the transition dynamics, the initial cluster configuration, and the embedding Euclidean space.

Found everywhere in nature, the intricate structures generated by fractal growth usually emerge from non-trivial self-organizing and self-assembling pattern formation^{1–4}. One striking feature of these systems is the morphological transition they undergo as a result of the interplay between entropic and energetic processes in their growth dynamics, that ultimately manifest themselves in the geometry of their structure⁵. It is here where, despite their complexity, great insight can be obtained into the fundamental elements of their dynamics from the powerful concepts of fractal geometry^{6,7}. Such is the case of the Laplacian growth or Dielectric Breakdown Model (DBM)^{8,9} that has importantly contributed to our understanding of far-from-equilibrium growth phenomena, to such an extent that seemingly unrelated patterns found in nature, such as river networks or bacterial colonies, are now understood in terms of a single framework of complex growth^{10,11}. Nonetheless, a complete scaling theory of growth far-from-equilibrium has been missing and, consequently, a comprehensive description of the fractality of systems that exhibit fractal to non-fractal morphological transitions as well^{7,12}.

Laplacian theory assumes that, in the absence of long-range interactions, the growth probability at a given point in space, μ , is generated by the spatial variation of a scalar field, ϕ , i.e., $\mu \propto |\nabla \phi|$. One example of such processes is the paradigmatic diffusion-limited aggregation (DLA) model, where particles performing a random walk aggregate one-by-one to form a cluster, starting from a seed particle (see Fig. 1). In particular, the structure that emerges from this process can be described by a single fractal dimension, D , only dependent on the Euclidean dimension of its embedding space, d . For the off-lattice two-dimensional ($d=2$) case, the corresponding fractal dimension has been widely reported to have a value $D = 1.71$ ¹². Furthermore, the theory has been extended to consider a more general and interesting growth process^{13–17} in which the mean-square displacement of the particles' trajectories, as the control parameter, generates a continuous morphological transition that can be neatly described through the fractal dimension of the walkers' trajectories, d_w . This transition goes from a compact cluster with $D=d$ for $d_w=1$, as expected for ballistic-aggregation (BA), to the DLA fractal for $d_w=2$ ¹⁸ (see Fig. 1).

However, one of the most challenging aspects of the theory arises when the growth is not purely limited by diffusion, e.g., when it takes place under the presence of long-range attractive interactions, where strong screening and anisotropic effects must be taken into account. In this case, the growth probability has been generalized

¹Instituto de Física, Benemérita Universidad Autónoma de Puebla, Puebla, 72570, Mexico. ²CIDS-Instituto de Ciencias, Benemérita Universidad Autónoma de Puebla, Puebla, 72570, Mexico. Correspondence and requests for materials should be addressed to J.L.C. (email: carrillo@ifuap.buap.mx)

Fractal to Non-Fractal Morphological Transitions in Stochastic Growth Processes

J.R. Nicolás-Carlock, V. Dossetti and

J.L. Carrillo-Estrada

Additional information is available at the end of the chapter



7

Abstract

8
9
10
11
12
13
14
15
16
17
18

From the formation of lightning-paths to vascular networks, diverse nontrivial self-organizing and self-assembling processes of pattern formation give rise to intricate structures everywhere and at all scales in nature, often referred to as fractals. One striking feature of these disordered growth processes is the morphological transitions that they undergo as a result of the interplay of the entropic and energetic aspects of their growth dynamics that ultimately manifest in their structural geometry. Nonetheless, despite the complexity of these structures, great insights can be obtained into the fundamental elements of their dynamics from the powerful concepts of fractal geometry. In this chapter, we show how numerical and theoretical fractal analyses provide a universal description to the well observed fractal to nonfractal morphological transitions in particle aggregation phenomena.

AQ01

19
20

Keywords: aggregation, entropic/energetic forces, fractal growth, morphological transitions, universality

21

1. Introduction

22
23
24
25
26

In nature, fractal structures emerge in a wide variety of systems as a local optimization of diverse growth processes restricted to the entropic and energetic inputs from the environment. Even more, the fractality of these systems determines many of their physical, chemical, and/or biological properties. Thus, to comprehend the mechanisms that originate and control the fractality is highly relevant in many areas of science and technology [1–3].

The fractal dimensions of Laplacian growth: an information entropy approach to self-similar cluster characterization

J. R. Nicolás-Carlock and J. L. Carrillo-Estrada*

Instituto de Física, Benemérita Universidad Autónoma de Puebla, Apdo. Postal. J-48, Puebla 72570, Mexico.

(Dated: June 5, 2017)

Laplacian growth is an ubiquitous out-of-equilibrium process of pattern formation able to generate a continuous set of fractal to non-fractal structures, including the paradigmatic diffusion-limited aggregation model within a particular scenario. However, a data-consistent analytical description of their fractality, valid beyond mean-field approximations, had been missing. Here we show that, an analytical solution to the fractality can be found by regarding the diffusion-limited growth as the maximum information-entropy production point in a dynamical model for the scaling of clusters undergoing a continuous morphological transition. Despite the complexity of the system, the solution found is an exclusive function of the Euclidean dimension of the embedding space and a characteristic growth-probability parameter. In particular, it provides a consistent characterization of data in two and three dimensions, and in general, is in excellent agreement with theoretical and numerical results for higher dimensions reported over the years.

The enormous diversity of fractal morphologies in nature is just matched by the great amount of out-of-equilibrium processes that generate them, making the issue of establishing an unified and comprehensive theory of fractal growth a great challenge [1–4]. However, it often happens that a simple model comes to unify diverse phenomena that once seemed to be completely unrelated. Such is the case of the Laplacian growth theory and its emblematic dielectric breakdown model (DBM), which constitute a paradigm of out-of-equilibrium growth that, due to its diversity of fractal morphologies, has received significant attention in diverse scientific and technological fields, from the oil industry, through bacterial growth, to even cosmology [5–7], with relevant applications in current neuroscience and cancer research [8–10]. Therefore, a precise characterization of this fundamental model in terms of its fractality is of the utmost importance.

In a generic growth process, the volume and surface of a given structure embedded in an Euclidean space of dimension d , can be described in terms of simple power-laws, $V \propto r^D$ and $dV/dr \propto r^\alpha$ respectively, where r is a characteristic radius, and D is the scaling or fractal dimension, with co-dimension $\alpha = D - 1$. In the DBM, the increment in volume is related to the growth probability distribution, $\sigma \propto |\nabla\phi|^\eta$, where ϕ is a scalar field associated to the energy landscape of the growing surface, and $\eta \geq 0$ is the growth probability parameter, a real number associated to the net effect of all non-linear interactions [11–20]. The most remarkable scenario of this model appears for $\eta = 1$, that corresponds to the well-known diffusion-limited aggregation (DLA) model, a stochastic particle aggregation process that generates dendritic structures for whom, D is only dependent on d (see Fig. 1a). This issue has been the subject of extensive research, not only for the well-known two-dimensional case, where $D = 1.71$ (from numerical [21–25] and theoretical [26–30] results), but for higher dimensions as well (although in this case, simulations [31–34] and theory

[35–41] are not in the best agreement).

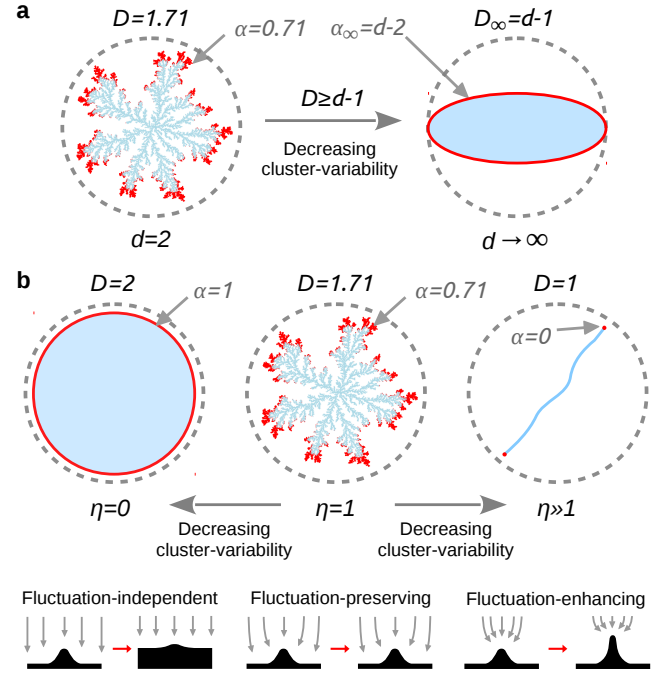


FIG. 1. **The Laplacian framework.** (a) Characteristic morphological and scaling features of the DLA fractal (with its cluster in blue and growing front in red), for $d = 2$ (left) and $d \rightarrow \infty$ (right) according to the Ball inequality, $D \geq d - 1$ [35]. (b) Characteristic features of the DBM for $d = 2$ and as function of η (top), with a generic description of the corresponding growth dynamics (as related to σ) at a small portion of the growing front (bottom).

In general, in terms of the fractal dimension $D(d, \eta)$, this model is characterized by a morphological transition from isotropic compact structures with $D_0 = d$ for $\eta = 0$ (Eden clusters), through intricate dendritic fractals with $1 < D < d$ (including DLA), to highly anisotropic linear structures as $\eta \gg 1$ (see Fig. 1b). Although with

important limitations, among the best analytical results for $D(d, \eta)$ there is the one provided by the mean-field approach [42–44],

$$D_{MF}(d, \eta) = \frac{d^2 + \eta(d_w - 1)}{d + \eta(d_w - 1)}, \quad (1)$$

where $d_w = 2$ is the fractal dimension of the random walkers' trajectories in any $d \geq 2$. This equations provides a good qualitative description of the η -transition, but fails to provide precise values for D (for example, $D_{MF}(\eta = 1) = 5/3 < 1.71$ in $d = 2$). Overall, despite all the previous results and observations, the derivation of a consistent analytical expression for $D(d, \eta)$, valid beyond mean-field approximations, has proven to be a non-trivial task and has been missing [4, 7] (see Fig. 2).

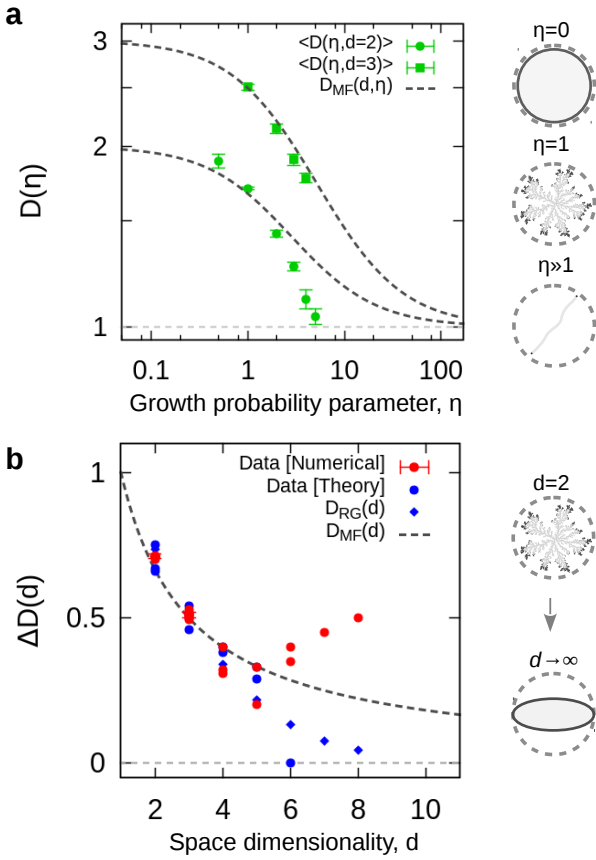


FIG. 2. DBM and DLA dimensions. (a) Numerical results (Table I) for $D(d, \eta)$ of the DBM for $d = 2$ and 3 in a log-log plot. (b) Numerical (red) and theoretical (blue) results (Table II) for $D(d, \eta = 1)$, expressed through $\Delta D = D - (d - 1)$, of the DLA model.

The mathematical model. Despite the complexity of the DBM morphological transition, a simple model can be established to describe its fractality by considering the fundamental elements of its growth dynamics, which are mainly two: *stochastic* and *energetic*. Qualitatively, as function of the growth parameter η , the growth dynamics

produce homogeneous stochastic growth for $\eta = 0$, fractal or unstable growth for $\eta \sim 1$, and highly anisotropic growth as $\eta \rightarrow \infty$ (see Fig. 1b). In terms of the fractality, this implies that as the energetic element is introduced in the stochastic growth dynamics, anisotropic or preferential growth is enhanced causing the fractal dimension of the clusters to decrease from its initial value $D_0 = d$, towards $D \rightarrow 1$ as $\eta \rightarrow \infty$. In this process, considering that all the information regarding the effects of stochastic/energetic growth-dynamics is encoded in an effective control parameter Γ , we define the dimension function $D(\Gamma)$, where $D(\Gamma) = D_0$ for $\Gamma = 0$ and $D(\Gamma) \rightarrow 1$ as $\Gamma \rightarrow \infty$, or in terms of the co-dimension, we have $\alpha(\Gamma) = D_0 - 1$ for $\Gamma = 0$ and $\alpha(\Gamma) \rightarrow 0$ as $\Gamma \rightarrow \infty$, correspondingly. Taking into account that the behaviour of D is smooth and monotonically decreasing as function of the control parameter, we may consider that its most general solution satisfies $dD/d\Gamma = d\alpha/d\Gamma < 0$, and therefore, it can be obtained from $d\alpha/d\Gamma = -f(\alpha)$. By expanding $f(\alpha)$ as a Taylor series up to the first-order term, $d\alpha/d\Gamma \approx -[f_0 + f_1\alpha + O(\alpha^2)]$, and by integrating between a given and finite α and Γ , i.e., $\int_{\alpha_0}^{\alpha} d\alpha'/(f_0 + f_1\alpha') = \int_0^{\Gamma} d\Gamma'$, we obtain,

$$D(\Gamma) = 1 + (D_0 - 1)e^{-\Gamma}, \quad (2)$$

where $f_0 = 0$ from the condition that $\alpha \rightarrow 0$ as $\Gamma \rightarrow \infty$, and f_1 has been absorbed in the effective control parameter Γ . From construction, Eq. (2) is the most general form for D , and the functional form of Γ must still be found. However, before proceeding to find it, let us now show why this equation is suitable to characterize this system by considering the DBM mean-field equation first.

The mean-field result given in Eq. (1) belongs to a special case of the family of equations given by Eq. (2). Starting with its first-order approximation in Γ , it follows that,

$$D^{(1)}(\Gamma) = 1 + \frac{D_0 - 1}{1 + \Gamma} = \frac{D_0 + \Gamma}{1 + \Gamma}. \quad (3)$$

Here, from direct comparison to Eq. (1), one observes that these expressions are equivalent, with Γ being nothing but $\Gamma_{MF} = \eta(d_w - 1)/d$, and $D_0 = d$. As previously commented, this equation does not provide the correct solution to D due to its mean-field nature, nonetheless, this example not only makes the relation between the effective parameter Γ and the actual parameter of the transition η more evident, but gives a clear picture of the generality of Eq. (2) as a fractality function. In order to find a suitable $\Gamma(d, \eta)$, specific conditions over D must be considered according to the DBM phenomenology, and particularly, a good insight can be found within the context of information theory as applied to out-of-equilibrium growth.

Special attention has been given to the entropy production rate of growing clusters as function of their ac-

tive front [45–47]. This is supported by the fundamental Turkevich-Scher conjecture, $D = 1 + \alpha^*$, that relates the fractal dimension of the cluster to the dimension of the most active region of its growing front, $\alpha^* = \alpha$, indicating that the scaling of the active perimeter, i.e., the co-dimension, contains the information needed to uniquely define the fractality of the cluster itself [7, 36]. A measure of this information, and the connection to entropy production, is found under the formalism of multifractal sets, where the information entropy, S , is related to the generalized dimension, D_q , through the first-order moment of the generalized Rényi entropies, $S_q = \log \sum_{i=1}^n p_i(\epsilon)^q / (q - 1)$, as, $D_{q=1} = \lim_{\epsilon \rightarrow 0} S_{q=1} / \log \epsilon$, where $S_{q=1} = -\sum_{i=1}^n p_i(\epsilon) \log p_i(\epsilon)$, and $p_i(\epsilon)$ is the probability of a given growth event at a spatial observation scale, ϵ [26]. In the case of self-similar structures, such as those characterizing the full DBM transition, the generalized dimension becomes independent of q , making all the fractal dimensions D_q (such as, box-counting $q = 0$, information $q = 1$, or correlation $q = 2$) equivalent and directly proportional to the information entropy, leading to $S(d, \eta) = kD(d, \eta) = k + k\alpha(d, \eta)$, with $k = \log \epsilon$. In terms of the entropy production, this relation implies that, for a fixed observation scale, $\partial S / \partial \eta = k\partial\alpha / \partial\eta \rightarrow 0$, for either $\eta \rightarrow 0$ or $\eta \gg 1$. In other words, the amount of information needed to characterize the active perimeter of a compact circular cluster as $\eta \rightarrow 0$, or the active tip of linear structures as $\eta \gg 1$, does not grow as much as the one needed to characterize the intermediate fractal perimeter of clusters at $\eta \sim 1$ (see Fig. 1b).

Under the previous observations, let us consider that this regime change in growth dynamics manifests itself in the fractality of the system as that point where $\partial^2 S / \partial \eta^2 = k\partial^2\alpha / \partial \eta^2 = 0$, this is, $\partial S / \partial \eta|_{\eta=\eta_i}$, becomes a global maximum. From Eq. (2), the inflection point η_i satisfies, $\partial^2\alpha / \partial \eta^2|_{\eta=\eta_i} = 0$, that translates into the inflection condition, $[(\partial\Gamma / \partial\eta)^2 - \partial^2\Gamma / \partial\eta^2]|_{\eta=\eta_i} = 0$. Then, to propose a suitable form for Γ , notice that in the mean-field case, the relation between parameters is linear, $\Gamma_{MF} = \eta/d$ (with d fixed), making it impossible to define $\eta_i > 0$. Therefore, we propose as a general *ansatz* for Γ ,

$$\Gamma(d, \eta) = \Gamma_0 \eta^\chi, \quad (4)$$

with $\Gamma_0 = \Lambda/d$, where Λ and χ are two positive real numbers that are associated with the strength of the effective growth forces. By applying the inflection condition to the new $\Gamma(d, \eta)$, we have that the regime-change of growth dynamics it satisfies $\Gamma_0 \eta_i^\chi = (\chi - 1)/\chi$, with $\chi \geq 1$. Then, in order to determine D , the parameters Λ and χ must be determined either numerically or theoretically. In the latter case, Eq. (2), along with Eq. (4), can be used as a fitting function to an available data set. In the former case, we can make use of a particular observation found in the angular correlation analy-

sis of DLA clusters which suggests that the DLA fractal ($\eta = 1$) can be associated to a critical dynamical state that defines the point of maximum entropy production [46–48]. In the case of our model, this is applied by setting $\eta_i = 1$, leading to $\chi = 1/(1 - \Gamma_0)$, and in this way, $\Gamma(d, \eta) = \Gamma_0 \eta^{1/(1-\Gamma_0)}$, where the solution to $D(d, \eta)$ is finally found once $\Lambda = \Lambda(d)$ is established. Notably, Γ is the specific term in $D(d, \eta)$ that keeps all the information regarding the fractality of the system. For example, for a given d , it is associated to the η -transition, and for $\eta = 1$, it is associated to the fractal dimensions of DLA across different Euclidean spaces. In fact, from Eq. (2), $\alpha(d, \eta) = (d - 1) \exp[-\Gamma(d, \eta)]$, is the function that provides all the information needed to define $D = 1 + \alpha$, as stated by the Turkevich-Scher conjecture.

Analytical solution for $\Gamma_0(d)$. Independently of the numerical or theoretical method to find Λ and χ , let us first notice that for $\eta = 1$, the dimensions $D(d, \eta)$ not only are associated to the fractal dimensions of DLA as an exclusive function of d , but are only dependent on the solution of $\Lambda = \Lambda(d)$. Once the solution to Λ is found for a fixed d , the straightforward procedure to obtain χ is by a linear fit to an available data-set plotted through, $\Gamma[D(\eta)] = -d \log[(D(\eta) - 1)/(d - 1)]$, that comes from Eq. (2). An alternative procedure is by directly using the hypothesis of maximum entropy production, for which $\chi = 1/(1 - \Gamma_0)$, with $\Gamma_0 = \Lambda/d$.

If the fractal dimensions of DLA are known for specific Euclidean spaces, one practical way to find Λ is by using Eq. (2) with $\eta = 1$ for which, $\Lambda[D(d)] = -d \log[(D(d)_{\eta=1} - 1)/(d - 1)]$. For example, in the two-dimensional DLA model, we have that $D_{\eta=1} = 1.71$, leading to $\Lambda_{d=2} = -2 \log(0.71) \approx 0.69$. Then, χ can be found by a linear fit to data plotted using $\Gamma[D(\eta)]_{d=2}$, for which $\chi = 1.36 \pm 0.02$; or by using the hypothesis of maximum entropy production, for which $\chi = 1/(1 - \Lambda_{d=2}/2) \approx 1.52$. This procedure can be applied to find Λ and χ for higher dimensions as long as there is available and reliable data to compute them. In Fig. 3a, we present the results of this analysis as applied for $d = 2$ and $d = 3$ (see also Table I and II). However, without prior knowledge of the DLA dimensions, here we show one way to find an analytical solution to $\Lambda(d)$.

The only analytical solution to $\Gamma_0(d)$ known so far, is that of the mean-field description, $\Gamma_{MF} = 1/d$, this is $\Lambda_{MF} = 1$. In general, $\Lambda(d)$ is expected to display a non-trivial behaviour as shown in Fig. 3b, where from Eq. (2), we applied $\Lambda[D(d)] = -d \log[(D(d) - 1)/(d - 1)]$, to all the available numerical results for $D(d)$ of Table II. In particular, we found that one way to construct this general $\Lambda(d)$ is by extending previous real-space renormalization-group (RG) results for on-lattice DLA [40, 41], to be valid in the continuous space. Under this RG approach, $D(k, d)_{RG} = 1 + \alpha(k, d) = 1 +$

$\log \mu(k, d) / \log 2$, with,

$$\mu(k, d) = 1 + 2 \binom{d-1}{1} \phi_1 + \sum_{k=2}^{d-1} \binom{d-1}{k} \phi_k, \quad (5)$$

where, $\phi_k(d)$ are the growth potentials for a given lattice, and $\mu(k, d)$ is inversely proportional to the maximum growth probability, $p(d)_{max} = \mu(k, d)^{-1} = 2^{-\alpha(k, d)}$.

One of the shortcomings of this model is its heavy dependence on a lattice, that makes it overestimate the well-known DLA dimension for $d = 2$, for example, it predicts $D_{RG} = 1.737$ for a square lattice. Nonetheless, by construction, it is able to provide a lower boundary to $\Lambda(d)$. In the $d \rightarrow \infty$ limit, $\phi_k \rightarrow 1/2$, leading to $\mu(d)_\infty = 2^{d-1} + d/2$, that establishes the lower boundary, $\Lambda^- = -d \log[\log \mu(d)_\infty / \log(2^{d-1})]$. An upper boundary can still be established from the Ball inequality, where $D \geq d - 1$, must be always satisfied, leading to, $\Lambda^+ = -d \log[(d-2)/(d-1)]$. Thus, a solution for $\Lambda(d)$ must be such that the inequality, $\Lambda^- \leq \Lambda(d) \leq \Lambda^+$, where the equality will hold for $d \rightarrow \infty$, should always be satisfied (see Fig. 3b). Under the previous considerations, the extension to continuous space, i.e., $\mu(k, d) \rightarrow \mu(d)$, is done by observing that when $d \rightarrow \infty$, all the information in $\mu(d)$ regarding $D(d \rightarrow 2)$ is lost, as seen through Λ^- . Then, without loss of generality, this information can be recovered by taking $\phi_k = 1/2$ (the limit-value of ϕ_k as $d \rightarrow \infty$) starting from $k \geq 2$. This leads to,

$$\mu(d) = 1 - d/2 + 2^{d-2} + 2(d-1)\phi(d), \quad (6)$$

where $\phi_1 \rightarrow \phi(d)$, is a continuous function of d . Now, as $d \rightarrow 2$, we have that $\phi(d) = (2^{D(d \rightarrow 2)-1} - 1)/2$, and $\mu(d) = 1 + 2\phi(d) = 2^{D(d \rightarrow 2)-1}$. These forms for $\phi(d)$ and $\mu(d)$, suggest that D can be approximated as, $D(d) - 1 \approx (d-1)/\sqrt{2}$, as $d \rightarrow 2$. Therefore, we propose the following ansatz for $\phi(d)$,

$$\phi(d) = (2^{\sqrt{(d-1)/2}} - 1)/d, \quad (7)$$

that along with $\mu(d)$, provides,

$$\Lambda(d) = -d \log[\log \mu(d) / \log 2^{d-1}], \quad (8)$$

and consequently, the solution for $\Gamma_0(d)$, see Fig. 3b. This solution satisfies the most rigorous restrictions imposed by the theory, and in particular, it predicts $D = 1 + 1/\sqrt{2} \approx 1.707$ for $d = 2$, in excellent agreement with the highly reported scaling of DLA. The complete solutions for $D(d, \eta)$ in $d = 2$ and $d = 3$, as well as $D(d)$ are shown in Figs. 3c and 3d, respectively.

Final remarks. Once an analytical solution to $D(d, \eta)$ has been found, an important issue to consider is that of the criticality of the DBM transition and its characterization using D as an order parameter, which for $d = 2$, it has been suggested that the full collapse to linear clusters occurs at critical value $\eta \approx 4$, although this criticality still needs of further clarification

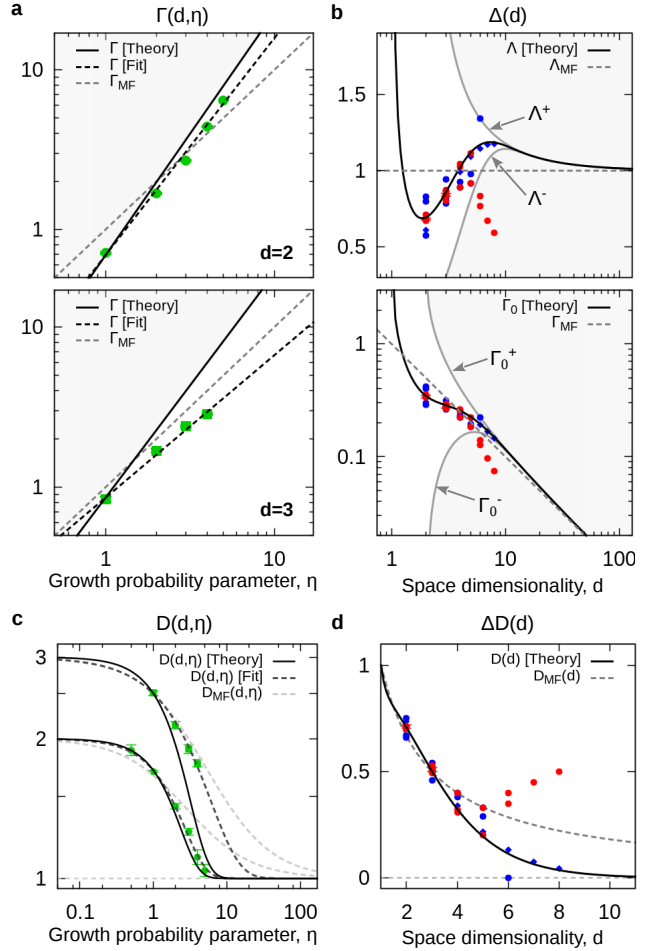


FIG. 3. DBM and DLA solutions. (a) Analysis of $\Gamma(d, \eta)$ in log-log plots for $d = 2$ (top) and $d = 3$ (bottom), using the data coming from Fig. 2a. Using Eq. (4) with $d = 2$, $\Lambda = 0.69$ with $\chi = 1.36 \pm 0.02$ from linear fit, and $\chi = 1.52$ from theory; for $d = 3$, $\Lambda = 0.84$ with $\chi = 0.91 \pm 0.02$ from linear fit, and $\chi = 1.39$ from theory. In the cases where the hypothesis of maximum entropy production, χ establishes the upper boundary for Γ . In the figures, the shaded regions indicate these forbidden regions. In both cases, $\Gamma_{MF} = \eta/d$ is shown. (b) The analytical solutions to $\Lambda(d)$ (top) and $\Gamma_0(d) = \Lambda(d)/d$ (bottom), as given by Eq. (8), are in great agreement with the data (coming from Fig. 2b) and theory. (c) Final theoretical and numerical solutions to $D(d, \eta)$ for $d = 2$ and $d = 3$. (d) The theoretical solution for $D(d)$, shown as $\Delta D = D - (d - 1)$. For the numerical values see Tables I and II.

[16, 49, 50]. To formally address this point, let us define the reduced co-dimension, $\hat{\alpha} = (D - 1)/(D_0 - 1)$, as the order parameter of the system, where $\hat{\alpha} \rightarrow 1$ as $D \rightarrow D_0$, and $\hat{\alpha} \rightarrow 0$ as $D \rightarrow 1$. From Eq. (2), given that $\hat{\alpha} = \exp[-\Gamma(d, \eta)]$ is a smooth function that tends to zero in a continuous manner, defining an specific point where it becomes exactly zero is not possible. This implies that, the previously suggested critical point for the DBM, i.e., the value for η where $D \approx 1$ [16], cannot be

treated as “critical” from the point of view of a formal critical phase-transition theory [46, 47]. Nevertheless, it is still possible to define a *transitional* point, η_t , i.e., a point where the highly screening/anisotropy effects are dominant over the morphology of the cluster. Mathematically, it can be defined from $D = 1 + \epsilon$, where $\epsilon \ll 1$, is the tolerance or deviation from $D = 1$, then from Eq. (2), $(\Lambda/d)\eta_t^\chi = -\log[\epsilon/(d-1)]$. For example, for $d = 2$ and using the theoretical value for χ , we have that $\eta_t(\epsilon = 0.05) \approx 4.1$ and $\eta_t(\epsilon = 0.10) \approx 3.5$, which are in great agreement with what it previously observed [16].

The most important outcome of this analysis is that of a complete numerical and analytical description for the fractal dimensions of the DBM, $D(d, \eta)$, given by Eqs. (2), (4) and (8), where the parameter χ was found under different numerical and analytical procedures. Particularly, by considering the hypothesis of maximum entropy production, a complete parameter-free description is obtained, that is in better agreement with the numerical results than the mean-field approximation. In the case of $\eta = 1$, that corresponds to the fractal dimensions of DLA, $D(d)$, we have a complete parameter-free analytical description that is in excellent agreement with reliable numerical and theoretical results reported over the years.

ACKNOWLEDGMENTS

Authors acknowledge partial financial support by CONACyT and VIEP-BUAP, grant CAREJ-EXC16-G.

* carrillo@ifuap.buap.mx; author to whom correspondence should be addressed.

- [1] Ben-Jacob, E. & Garik, P. The formation of patterns in non-equilibrium growth. *Nature* **343**, 523 (1990).
- [2] Ben-Jacob, E. From snowflake formation to growth of bacterial colonies II: Cooperative formation of complex colonial patterns. *Contemp. Phys.* **38**, 205 (1997).
- [3] T. Vicsek, *Fractal Growth Phenomena* (World Scientific, Singapore, 1992).
- [4] P. Meakin, *Fractals, Scaling and Growth Far from Equilibrium* (Cambridge University Press, Cambridge, 1998).
- [5] Sander, L. M. Fractal growth processes. *Nature* **322**, 789 (1986).
- [6] Sander, L. M. Diffusion-limited aggregation: a kinetic critical phenomenon? *Contemp. Phys.* **41**, 203 (2000).
- [7] Sander, L. M. Fractal Growth Processes, in *Mathematics of Complexity and Dynamical Systems*, 2011, edited by R. A. Meyers (Springer, New York, 2011), p. 429.
- [8] Sturmberg, J. P. & West, B. J., Fractals in Physiology and Medicine. in *Handbook of Systems and Complexity in Health* (ed. Sturmberg, J. P. & Martin, C. M.) pp. 171–192 (Springer New York, 2013).
- [9] Lennon, F. E. et al. Lung cancer—a fractal viewpoint. *Nat. Rev. Clin. Oncol.* **12**, 664–675 (2015).

- [10] Di Ieva, A. The Fractal Geometry of the Brain. *Springer series in computational neuroscience*, edited by A. Di Ieva (Springer, 2016).
- [11] Niemeyer, L., Pietronero, L. & Wiesmann, H. J. Fractal Dimension of Dielectric Breakdown. *Phys. Rev. Lett.* **52**, 1033 (1984).
- [12] Hayakawa, Y., Kondo, H. & Matsushita, M. Monte Carlo Simulations of the Generalized Diffusion-Limited Aggregation. *J. Phys. Soc. Jpn.* **55**, 2479–2482 (1986).
- [13] Pietronero, L., Erzan, A. & Everts, C. Theory of Fractal Growth. *Phys. Rev. Lett.* **61**, 861 (1988).
- [14] Amitrano, C. Fractal dimensionality for the η model. *Phys. Rev. A* **39**, 6618 (1989).
- [15] Sanchez, A., Guinea, F., Sander, L.M., Hakim, V., & Louis, E. Growth and forms of Laplacian aggregates. *Phys. Rev. E* **48**, 1296 (1993).
- [16] Hastings, M. B. Fractal to Nonfractal Phase Transition in the Dielectric Breakdown Model. *Phys. Rev. Lett.* **87**, 175502 (2001).
- [17] Somfai, E., Goold, N. R. & Ball, R. C. Growth by random walker sampling and scaling of the dielectric breakdown model. *Phys. Rev. E* **70**, 051403 (2004).
- [18] Tolman, S. & Meakin, P. Two-, three- and four-dimensional diffusion-limited aggregation models. *Phys. A* **158**, 801 (1989).
- [19] Satpathy, S. Dielectric breakdown in three dimensions: results of numerical simulations. *Phys. Rev. B* **33**, 5093 (1986).
- [20] Vespignani, A. & Pietronero, L. Fixed scale transformation applied to diffusion limited aggregation and dielectric breakdown model in three dimensions. *Phys. A* **173**, 1 (1993).
- [21] Hinrichsen, E. L. et al. Self-similarity and structure of DLA and viscous fingering clusters. *J. Phys. A: Math. Gen.* **22**, L271 (1989).
- [22] Ossadnik, P. Multiscaling analysis of large-scale off-lattice DLA. *Phys. A* **176** 454–462 (1991).
- [23] Mandelbrot, B., Kol, B. & Aharoni, A. Angular Gaps in Radial Diffusion-Limited Aggregation: Two Fractal Dimensions and Nontransient Deviations from Linear Self-Similarity. *Phys. Rev. Lett.* **88** 055501 (2002).
- [24] Alves, S. G., Ferreira Jr., S. C. Aggregation in a mixture of Brownian and ballistic wandering particles. *Phys. Rev. E* **73**, 051401 (2006).
- [25] Menshutin, A. Scaling in the Diffusion Limited Aggregation Model. *Phys. Rev. Lett.* **108** 015501 (2012).
- [26] Halsey, T. C., Meakin, P. & Procaccia, I. Scaling Structure of the Surface Layer of Diffusion-Limited Aggregates. *Phys. Rev. Lett.* **56**, 854 (1986).
- [27] Nagatini, T. A renormalisation group approach to the scaling structure of diffusion-limited aggregation. *J. Phys. A* **20**, L381 (1987).
- [28] Hastings, M. B. Renormalization theory of stochastic growth. *Phys. Rev. E* **55**, 135 (1997).
- [29] Hayakawa, Y. & Sato, S. Statistical Theory of Diffusion-Limited Growth in Two Dimensions. *Phys. Rev. Lett.* **79**, 95 (1997).
- [30] Davidovitch, B., Jensen, M., Levermann, A., Mathiesen, J. & Procaccia, I. Thermodynamic Formalism of the Harmonic Measure of Diffusion Limited Aggregates: Phase Transition *Phys. Rev. Lett.* **87** 164101 (2001).
- [31] Meakin, P. Diffusion-controlled cluster formation in two, three, and four dimensions. *Phys. Rev. A* **27**, 604 (1983).

TABLE I. **DBM dimensions.** The average dimension, $\langle D(d, \eta) \rangle$, for $d = 2$ [13, 14, 16–18] and $d = 3$ [18–20] is compared to $D(d, \eta)_{MF}$ and $D(d, \eta)$ as obtained by the theory (T) and by a direct fit (F) to data (see Fig. 3). For $d = 3$, the fit results give a $\chi < 1$ that does not satisfy the inflection condition $\chi \geq 1$. Full data set available in Supplementary Materials.

Source	Λ	χ	$\eta = 0.5$	$\eta = 1$	$\eta = 2$	$\eta = 3$	$\eta = 4$	$\eta = 5$	η_i
$\langle D(\eta, d = 2) \rangle$			1.89 ± 0.05	1.70 ± 0.01	1.43 ± 0.02	1.26 ± 0.02	1.11 ± 0.04	1.04 ± 0.03	
$D(\eta, d = 2)$ (F)	0.69	1.36 ± 0.02	1.87	1.71	1.41	1.22	1.10	1.05	≈ 0.8
$D(\eta, d = 2)$ (T)	0.69	1.52	1.88	1.71	1.37	1.16	1.06	1.02	1.0
$D_{MF}(\eta, d = 2)$	1.0	1.0	1.80	1.67	1.50	1.40	1.33	1.29	—
$\langle D(\eta, d = 3) \rangle$				2.51 ± 0.03	2.14 ± 0.04	1.90 ± 0.04	1.77 ± 0.03		
$D(\eta, d = 3)$ (F)	0.84	0.91 ± 0.02		2.51	2.18	1.93	1.74		—
$D(\eta, d = 3)$ (T)	0.84	1.39		2.51	1.96	1.55	1.29		1.0
$D_{MF}(\eta, d = 3)$	1.0	1.0		2.50	2.20	2.00	1.86		—

TABLE II. **DLA dimensions.** First section: numerical results for $D(d, \eta = 1)$ with the corresponding average, $\langle D(d) \rangle$. Clusters grown off-lattice marked with ‘*’, while the rest are for a square lattice. Second section: theoretical results are compared to $D(d)_{MF}$ and $D(d)$ obtained by the theory (T). Error in measurements shown when available.

Source	$d = 2$	$d = 3$	$d = 4$	$d = 5$	$d = 6$	$d = 7$	$d = 8$
Rodriguez & Sosa [34]	$1.711 \pm 0.008^*$	$2.51 \pm 0.01^*$					
Meakin [31, 32]	$1.71 \pm 0.07^*$	$2.50 \pm 0.08^*$					
	1.71 ± 0.05	2.51 ± 0.06	3.32 ± 0.10				
	1.70 ± 0.06	2.53 ± 0.06	3.31 ± 0.10	4.20 ± 0.16	≈ 5.35		
Tolman & Meakin [33]	$1.715 \pm 0.004^*$	2.495 ± 0.005	≈ 3.40	≈ 4.33	≈ 5.40	≈ 6.45	≈ 7.50
$\langle D(d) \rangle$	1.71 ± 0.01	2.51 ± 0.01	3.34 ± 0.05	4.27 ± 0.09	5.38 ± 0.04	—	—
Turkevich & Scher [36]	1.67	2.46					
Erzan, <i>et al.</i> [37]	1.71	2.54					
Halsey [38]	1.66	2.50	3.40	4.33			
Hentschel [39]	1.75	2.52	3.38	4.29	5.0		
$D(d)_{RG}$ [40, 41]	1.74	2.52	3.34	4.22	5.13	6.08	7.05
$D(d)$ (T)	1.71	2.50	3.32	4.12	5.11	6.07	7.04
$D(d)_{MF}$	1.67	2.50	3.40	4.33	5.29	6.25	7.22

- [32] Meakin, P. Diffusion-controlled cluster formation in 2-6 dimensional space. *Phys. Rev. A* **27**, 1495 (1983).
- [33] Tolman, S. & Meakin, P. Off-lattice and hypercubic-lattice models for diffusion-limited aggregation in the dimensionalities 2-8. *Phys. Rev. A* **40**, 428 (1989).
- [34] Rodriguez-Romo, S. & Sosa-Herrera, A. Lacunarity and multifractal analysis of the large DLA mass distribution. *Phys. A* **392** 3316 (2013).
- [35] R. C. Ball and T. A. Witten, Particle Aggregation versus Cluster Aggregation in High Dimensions. *J. Stat. Phys.* **36**, 873 (1984).
- [36] Turkevich, L. A. & Scher, H. Occupancy-Probability Scaling in Diffusion-Limited Aggregation. *Phys. Rev. Lett.* **55**, 1026 (1985).
- [37] Erzan, L., Pietronero, L. & Vespignani, A. The fixed-scale transformation approach to fractal growth. *Rev. Mod. Phys.* **67** 545 (1995).
- [38] Halsey, T. C., Diffusion-Limited Aggregation as Branched Growth. *Phys. Rev. Lett.* **72**, 1228 (1994).
- [39] Hentschel, H. G. E. Fractal dimension of Generalized Diffusion-Limited Aggregates. *Phys. Rev. Lett.* **52**, 212 (1984).
- [40] Wang, X. R., Shapir, Y. & Rubinstein, M. Kinetic renormalization group approach to diffusion limited aggregation. *Phys. Lett. A* **138**, 274 (1989).
- [41] Wang, X. Z. & Huang, Y. Calculation of the fractal dimension of diffusion-limited aggregation by the normalisation-group approach in an arbitrary Euclidean dimension d . *Phys. Rev. A* **46** 5038 (1992).
- [42] Muthukumar, M. Mean-Field Theory for Diffusion-Limited Cluster Formation. *Phys. Rev. Lett.* **50**, 839 (1983).
- [43] Tokuyama, M. & Kawasaki, K. Fractal dimensions for diffusion-limited aggregation. *Phys. Lett.* **100A**, 337 (1984).
- [44] Matsushita, M., Honda, K., Toyoki, H., Hayakawa, Y. & Kondo, H. Generalization and the Fractal Dimensionality of Diffusion-Limited Aggregation. *J. Phys. Soc. Jpn.* **55**, 2618–2626 (1986).
- [45] Kaufman, J. H., Melroy, O. R. & Dimino, G. M. Information-theoretic study of pattern formation: Rate of entropy production of random fractals. *Phys. Rev. A* **39**, 1420 (1989).

- [46] Kaufman, J. H. & Dimino, G. M. Information-theoretic specific heat of fractal patterns. *Phys. Rev. A* **39**, 6045 (1989).
- [47] Dimino, G. M. & Kaufman, J. H. Evidence of critical behavior in a random fractal automaton. *Phys. Rev. Lett.* **62**, 2277 (1989).
- [48] Gleiser, M. & Sowinski, D. Information-entropic signature of the critical point. *Phys. Lett. B* **747**, 125 (2015).
- [49] Mathiesen, J. & Jensen, M. H. Tip Splitting and Phase Transitions in the Dielectric Breakdown Model: Mapping to the Diffusion-Limited Aggregation Model. *Phys. Rev. Lett.* **88**, 235505 (2002).
- [50] Mathiesen, J., Jensen, M. H. & Bakk, J. Ø. H. Dimensions, maximal growth sites, and optimization in the dielectric breakdown model. *Phys. Rev. E* **77**, 066203 (2008).



BUAP

MEMORANDUM

Para:	Dra. Minerva González Melchor, (Presidente) Dr. José Elías López Cruz. Dr. Emerson L. Sadurní Hernández. Dr. José Luis E. Carrillo Estrada, (Asesor).
De:	Dr. Antonio Flores Riveros, Coordinador del área de Física.
Asunto:	Inicia la revisión de la tesis de Doctorado del M.C. José Roberto Nicolás Carlock (DCF).
Fecha:	Lunes 08 de mayo, 2017.
Anexo:	Tesis en formato pdf Artículo(s) publicado(s)en formato pdf Formato para el dictamen de revisión

Me permito informarles que el Comité Académico del IFUAP, los ha designado integrantes del Comité Revisor de la Tesis de Doctorado en Ciencias (Física) del **M.C. José Roberto Nicolás Carlock**, para tal efecto anexo en formato pdf la tesis cuyo título es: ***"Universalidad de transiciones morfológicas en procesos de crecimiento estocásticos"***. Se les informa que se invitará a participar al Dr. Gerardo García Naumis, en calidad de examinador externo.

De acuerdo con nuestro reglamento de posgrado el plazo máximo para la revisión de la tesis es de 4 semanas, les pido hagan llegar en el formato anexo su dictamen de revisión al correo: fperez@ifuap.buap.mx

La fecha para la entrega de su evaluación será el día: **06 DE JUNIO DE 2017.**

Dr. Antonio Flores Riveros
Coordinador

Instituto de Física
"Ing. Luis Rivera
Terrazas"

Av. San Claudio esq. 18 sur, edif 110 A, B y C.
Ciudad Universitaria, Col. San Manuel,
Puebla, Pue. C.P. 72570
01(222) 2295610, Fax: ext. 5611